[American Journal of Science, Vol. 319, October, 2019, P. 658-693, DOI 10.2475/08.2019.02]

GEOCHEMISTRY OF INTRUSIVE ROCKS ON THE PRESCOTT PENINSULA, CENTRAL MASSACHUSETTS, USA: IMPLICATIONS FOR LATE DETACHMENT FAULTING WITHIN THE ORDOVICIAN TACONIAN VOLCANIC ARC

KURT HOLLOCHER*,†, PETER ROBINSON**, BENJAMIN LUCAS***, and STEPHEN MABEE§

ABSTRACT. The Prescott Peninsula contains two intrusive bodies: the Cooleyville Gneiss (449 Ma) and the Packard Gabbro (407 Ma), which cuts the Cooleyville. These are centrally located in the Bronson Hill Anticlinorium, a complex structural belt in western New England that includes metamorphosed rocks of the Ordovician Taconian arc plutonic complex (TAPC), and associated metamorphosed volcanic rocks. TPAC gneisses (locally 454–442 Ma) are overlain by stratified units including the Ordovician Ammonoosuc Volcanics (locally 453 Ma), Partridge Formation (locally 449 Ma), and several Silurian and Devonian units.

The Cooleyville Gneiss and Packard Gabbro are both calc-alkaline and have similar, arc-associated geochemical anomalies expressed in multi-element diagrams. These units are chemically distinct from several regionally exposed Devonian plutons, but are almost identical to plutonic rocks of the TAPC. The Cooleyville Gneiss cuts the Ammonoosuc Volcanics and Partridge Formation, but the TAPC does not, at least over extensive regions. Additionally, the Ammonoosuc Volcanics and Partridge Formation are each in contact with the TAPC in different areas: Partridge Formation locally to the east and west, and Ammonoosuc Volcanics in a central belt.

A multi-part model explains these relationships: 1) The Cooleyville Gneiss is part of the TAPC, having intruded the Ammonoosuc Volcanics and Partridge Formation east of the main arc axis. 2) Following arc collision with Laurentia, extensive detachment faulting decapitated the TAPC and Cooleyville pluton, sliding them and adjacent units west and down. 3) A second detachment carried part of the Ammonoosuc and Partridge farther west, completing the observed contact geographic pattern. 4) Following isostatic readjustment, erosion, and cooling, Silurian and Devonian units were deposited, in part unconformably on the TAPC. 5) Early Acadian (Devonian) subduction beneath composite Laurentia produced extensive central New England magmatism, and reactivated remnant Taconian lithospheric mantle beneath the TAPC, producing the Packard Gabbro and age-equivalent volcanics in the nearby Erving Formation.

Detachment faulting is common in arc and collisional settings. This model of late Taconian detachment faulting appears to solve a long-standing problem understanding the TAPC contact with overlying Ordovician units.

Key words: Prescott Peninsula, Quabbin Reservoir, Packard Gabbro, Cooleyville Gneiss, igneous geochemistry, Erving Formation, detachment fault, geologic map

INTRODUCTION

Overview

Volcanic arc–continent collision zones are common in orogenic belts throughout the world. Their development has been elucidated mostly using modern or older, relatively intact examples. Ancient collisional belts, particularly those strongly affected

* Geology Department, Union College, 807 Union Street, Schenectady, New York 12308, USA
** Geological Survey of Norway, Trondheim, N-7491, Norway, deceased
*** 8 Berrybrook Cr., Chappaqua, New York 10514, USA
§ Massachusetts Geological Survey, University of Massachusetts, 627 North Pleasant Street, Amherst, Massachusetts 01003, USA
† Corresponding author: hollochk@union.edu

by subsequent erosion and metamorphism, are more difficult to unravel because much of the original evidence has been lost or strongly modified. We present the results of a decades-long effort to understand a set of seemingly contradictory structural, tectonostratigraphic, and intrusive relationships in the Taconian volcanic arc of southern New England. The Taconian arc collided with Laurentia in the Ordovician, and was then strongly metamorphosed in the Early Devonian Acadian Orogeny, with regional metamorphism and pluton emplacement sporadically continuing through the Late Devonian to Early Mississippian Neo-Acadian episode, and ending in the Alleghenian (for example, Robinson and others, 1998; Wintsch and others, 2003; van Staal and others, 2009; Massey and others, 2017). This study applies igneous rock geochemistry, previously published geochronological results, new map compilation and reinterpretation, and recent developments in understanding continental arcs and collisional orogens, to help solve a long-standing problem regarding late-stage development of the Taconian arc complex.

Background

The Appalachian orogenic belt is a composite of several segments that were accreted to Laurentia in the Paleozoic. In southern New England, the tectonic architecture includes (fig. 1, from west to east): 1) Middle Proterozoic Laurentian basement that is overlain by Cambrian and Ordovician platform and margin sediments. 2) Ordovician Taconic allochthons of the Taconian arc accretionary wedge, with exposed thrust slices of Laurentian crust. 3) The Taconian igneous arc itself, most prominently exposed as its metamorphosed plutonic roots in the Bronson Hill anticlinorium, generally assigned to the western margin of the Central Maine Belt. 4) The deep basin of the Central Maine Belt, mostly overlain by metamorphosed Silurian and Devonian sedimentary rocks, but locally exposing Late Proterozoic, Cambrian, and Ordovician rocks, commonly assigned to the Ganderia segment of Gondwana. 5) The Nashoba terrane, a Cambrian–Ordovician arc complex probably developed on the eastern Ganderian margin. 6) The mostly Late Proterozoic Gondwanan Avalon terrane. During and following successive accretion of these segments onto Laurentia, there was a complex sequence of deformation, metamorphism, and igneous activity that extended into the Permian. This summary is based largely on Stanley and Ratcliffe (1985), Osberg and others, (1989), Sevigny and Hanson (1993), Robinson and others (1998), Tucker and others (2001), Robinson (2003), Tremblay and Pinet (2005), Thompson and others (2012), Kay and others (2017), and Massey and others (2017).

Igneous rocks on the Prescott Peninsula (fig. 2) include the Cooleyville Gneiss and Packard Gabbro, occurring in the west-overturned, isoclinal Prescott Syncline, in the middle of the Taconian arc plutonic complex (TAPC) as exposed in the Bronson Hill anticlinorium. The area surrounding the Prescott Peninsula was mapped by Robinson (ms, 1963). Most of the Peninsula itself was mapped by Makower (ms, 1964), who used the term Prescott Complex to include both the gneiss and gabbro. This term was also used in the Bedrock Geologic Map of Massachusetts (Zen, 1983), and elsewhere. The intrusions were assumed to be cogenetic, and Devonian (Acadian), because the northwestern part of the Cooleyville Gneiss was interpreted to intrude the Ordovician Ammonoosuc Volcanics and Partridge Formation, the Silurian Clough Quartzite, and the Early Devonian Littleton Formation in the Prescott Syncline, and assumed to be related to widespread Devonian magmatism in southern New England. Two zircon U–Pb radiometric ages were published by Tucker and Robinson (1990), 449 +5/−3 Ma for the Cooleyville Gneiss (Ordovician) and 407 +3/−2 Ma for the Packard Gabbro (Devonian), making the concept of a cogenetic Prescott Complex untenable.

Reconsideration of the original and more recent mapping, available age dates, new geochemical data, and a complete re-working of field notes, led to the new map

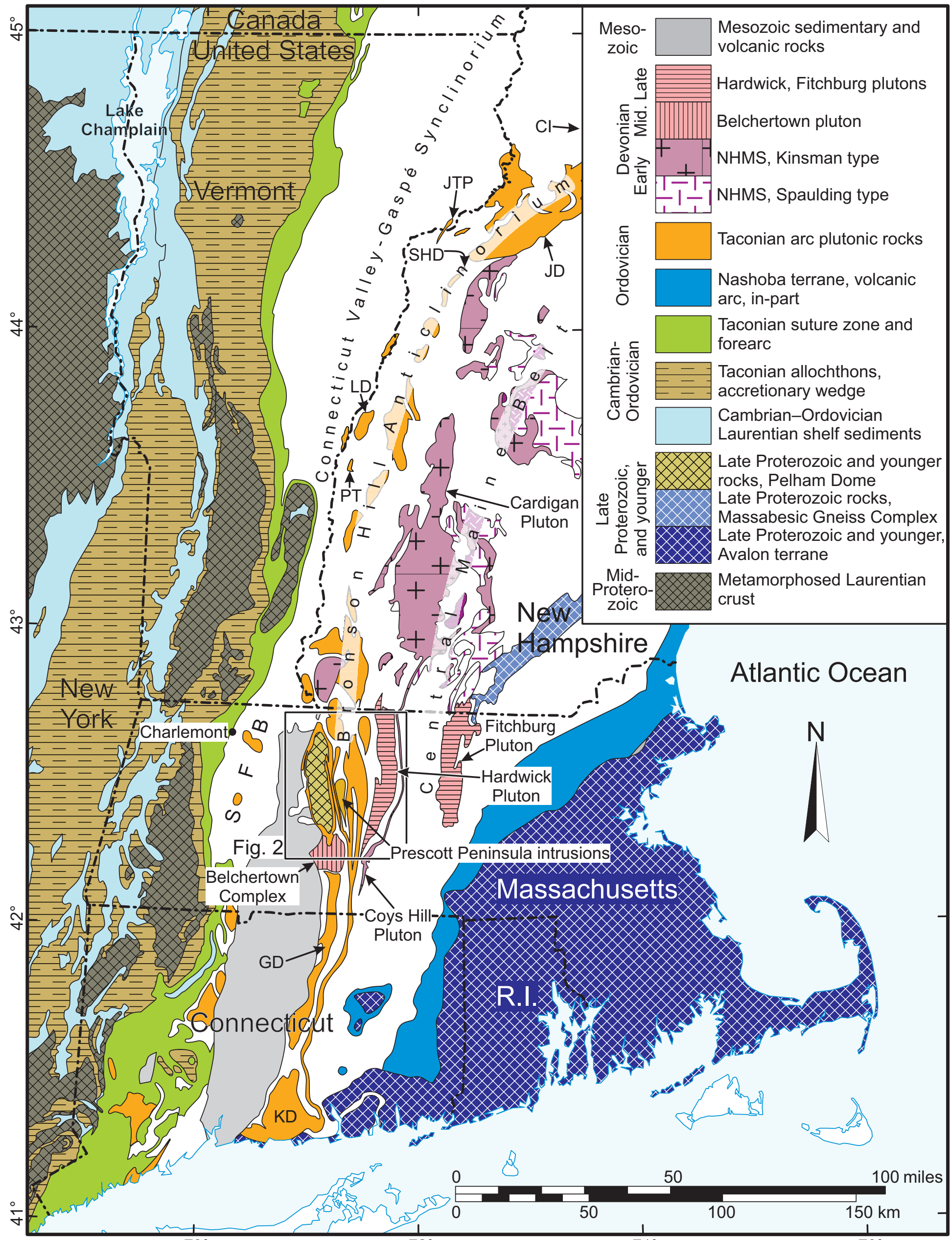

Fig. 1. Simplified lithotectonic map of southern New England and eastern New York. Emphasized are structures related to the Taconian Orogeny, plutonic rocks related to Early Devonian subduction of Iapetus crust attached to Avalon (Acadian Orogeny), and the Late Devonian Hardwick Pluton and Middle Devonian Belchertown Complex, both used in our comparison data sets. White areas are undifferentiated metamorphosed stratified rocks (mostly Ordovician–Devonian), and plutonic rocks (mostly Silurian–Cretaceous). Adapted from Zen (1983), Lyons and others (1997), Dorais (2003), and Hibbard and others (2006). CI, Chickwolnepy intrusions; GD, Glastonbury Dome; JD, Jefferson Dome; JTP, Joslin Turn Pluton; KD, Killingworth Dome; PT, Plainville Tonalite; SFB, Shelburne Falls Belt, containing metamorphosed Taconian arc plutonic and volcanic rocks; SHD, Sugar Hill Dome; LD, Lebanon Dome.

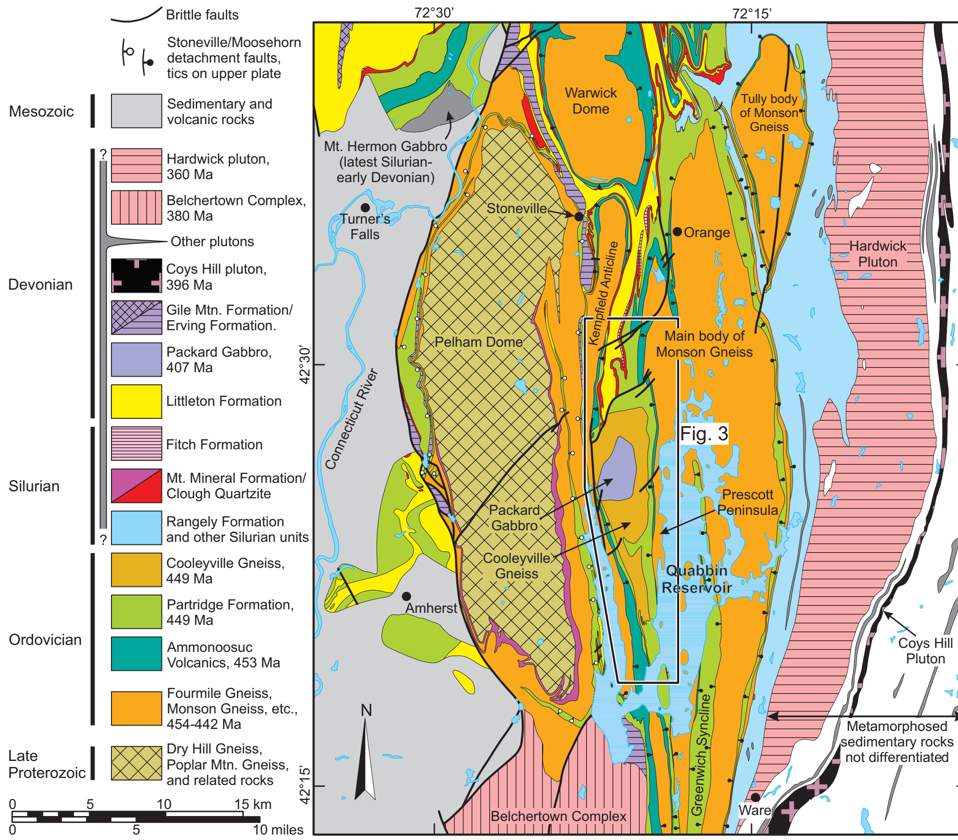

Fig. 2. Simplified geologic map of north-central Massachusetts, showing the region around the Prescott Peninsula, containing the Ordovician Cooleyville Gneiss and Devonian Packard Gabbro. See text for radiometric age sources. Adapted from Zen (1983), Elbert and others (1988), and Robinson (2009, 2011, 2012, 2017).

(fig. 3). Locally, the main change to the map was the northwestern contact of the Cooleyville Gneiss, previously interpreted as intrusive into all stratified units, but now interpreted to be a Mesozoic brittle normal fault. The fault is a new segment connecting the previously mapped New Salem Faults to the northeast, and the Lighthouse Hill Fault to the southwest.

The body of Cooleyville Gneiss is about 17.5 km long, north to south, 3.6 km wide at its north end, and less than 100 m wide at its extended, southernmost end, covering about 23 km^2. The Cooleyville Gneiss intrudes adjacent Ordovician stratified rocks of the Ammonoosuc Volcanics and Partridge Formation, both containing Taconian volcanic rocks, dated at 453 ± 2 and 449 $+3/-2$ Ma, respectively (Tucker and Robinson, 1990). The gneiss is intruded by one large and several smaller bodies of Packard Gabbro in the north-central part, covering about 7 km^2 in total. The bodies of Packard Gabbro are almost entirely enclosed within the Cooleyville Gneiss, but one small body cuts the Partridge Formation. The Prescott Syncline, in which the intrusive rocks are emplaced, is flanked to the west by Monson Gneiss of the Kempfield Anticline, and to the east by the Main Body of Monson Gneiss. The Monson Gneiss and nearby, essentially identical Fourmile Gneiss of the Pelham Dome (fig. 2, west side of fig. 3), represent the locally exposed plutonic roots of the TAPC (Hollocher and

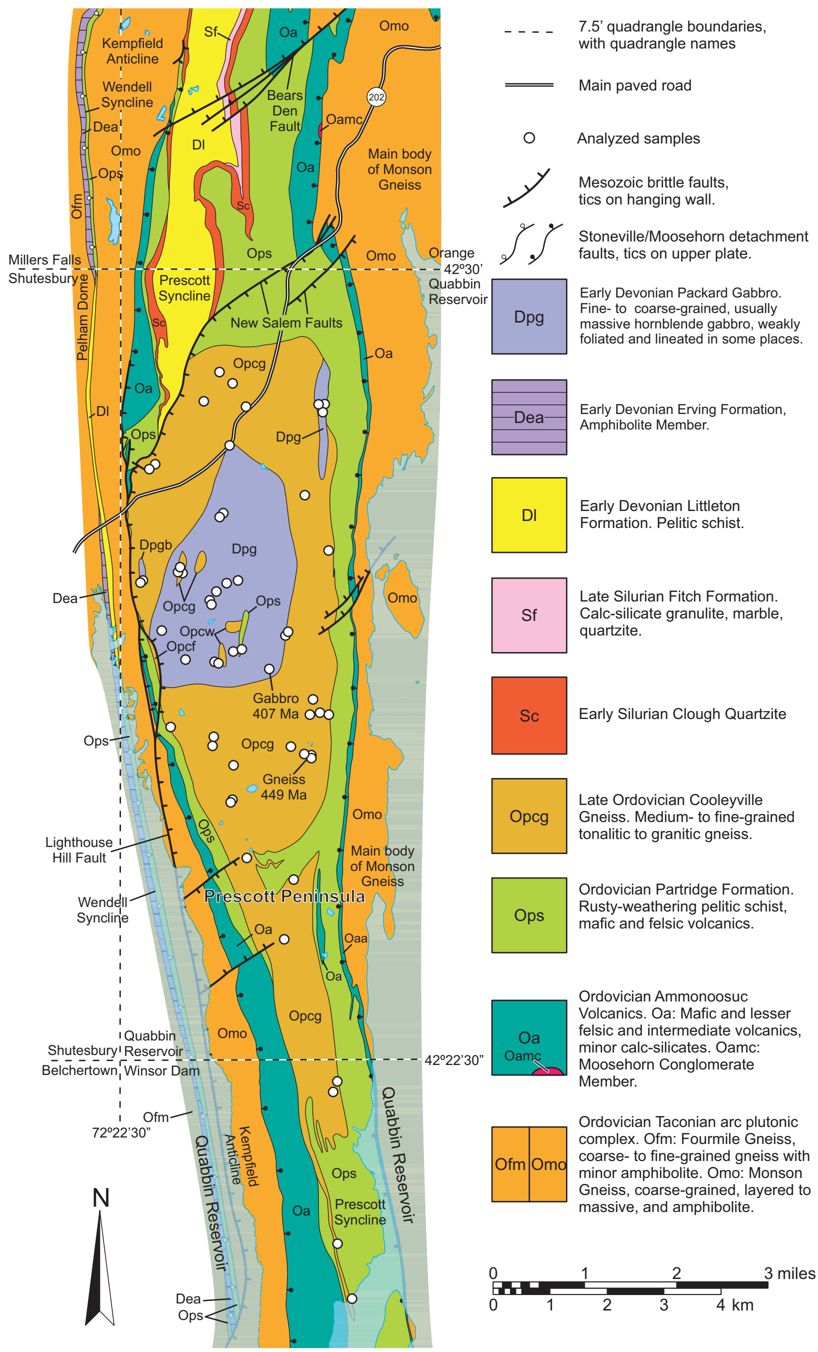

Fig. 3. New geologic map of the Prescott Peninsula and its surroundings (simplified), showing sample locations for Cooleyville Gneiss and Packard Gabbro (see table A2, Appendix, for sample numbers, coordinates, and descriptions; see fig. A1 for fully-detailed map and unit descriptions).

others, 2002). They, and similar rocks in the area of figure 2, range in age from 454 +3/−2 to 442 +3/−2 Ma (Tucker and Robinson, 1990; Karabinos and others, 2017; 11 total samples). Over the length and breadth of the Taconian arc complex, TAPC and apparently related metamorphosed intrusive and volcanic rocks span a range of 477 to 441 Ma (Zartman and Leo, 1985; Lyons and others, 1986; Aleinikoff and Moench, 1987; Tucker and Robinson, 1990; Moench and others, 1995; Karabinos and others, 1998, 2017; Moench and Aleinikoff, 2003; Rankin and others, 2013; Valley and Walsh, 2013; Aleinikoff and others, 2015; Valley and others, 2015; Walsh and others, 2017).

Plutonic Rock Types

The Cooleyville Gneiss is comprised mainly of light-gray to yellow-weathering, fine- to medium-grained, generally foliated and weakly-lineated felsic gneiss, ranging from tonalitic to granitic. The gneisses all contain biotite, most contain epidote, and muscovite or hornblende occur in some places. Garnet is rare. Muscovite tends to be abundant near contacts with the Partridge Formation, particularly on the eastern side of the body, suggestive of an intrusive contact and magmatic contamination. Intrusive relationships include Cooleyville Gneiss cutting Ammonoosuc Volcanics and Partridge Formation contacts in the southern part of the body, and by the presence of inclusions of rusty-weathering Partridge Formation schist in the gneiss (Makower, ms, 1964; fig. 3). Some exposures have irregular distributions of more mafic patches, a few centimeters to a meter long, that appear to be deformed xenoliths (fig. 4A).

The Packard Gabbro ranges from fine-grained in most of the body, to very coarse (fig. 4B), and is usually equigranular. The gabbro seems less-deformed than the Cooleyville Gneiss, but some outcrops were locally foliated (fig. 4C), possibly in discrete shear zones. Biotite can be abundant, but garnets are rare. Two unusually quartz-rich gabbro exposures contain abundant, large garnets (sample 2I1b up to 2 cm across, and 2F8 up to 5 cm, fig. 4D). No pyroxene was seen in the field or in thin section, but Makower (ms, 1964) and we observed several samples with single hornblende crystals up to 5 mm across, poikilitic with plagioclase, that contained abundant, tiny Fe–Ti oxide inclusions that may have unmixed from former magmatic pyroxene or hornblende. These large crystals are set in a matrix of 0.5 to 1 mm, oxide-free hornblende and plagioclase. The large hornblendes texturally resemble poikilitic pyroxene or hornblende crystals common in gabbroic cumulates.

Both the Cooleyville Gneiss and Packard Gabbro differ in grain size and mineral proportions between outcrops, and even in single outcrops. This suggests that both bodies were not emplaced as large, single magmatic masses, but rather are composites of many small intrusions. The better-exposed Main body of Monson Gneiss, to the east, gives a similar impression in the field (for example, Hollocher and others, 2002).

SAMPLE SETS AND PROCEDURES

From the Prescott Peninsula we present 32 new whole-rock chemical analyses of Cooleyville Gneiss, and 29 of Packard Gabbro. We also include 10 new analyses of amphibolites from the nearby and possibly related Devonian Erving formation, and new data on several other local, metamorphosed plutonic bodies. Sample set descriptions, sample locations and descriptions, and new data are given in tables A1, A2, and A3, respectively (Appendix, http://earth.geology.yale.edu/%7eajs/SupplementaryData/2019/Hollocher). Thin sections were made of about half of the samples, and were examined using polarized light microscopy. New samples weighed 1 to 10 kg. They were cleaned, weathered parts split off, and the remainder crushed in a hydraulic press with tungsten carbide faces to pass a 6 mm stainless steel sieve. 50 gram splits were powdered in a Spex® aluminum oxide puck mill. All new analyses were done using the procedures of Hollocher and others (2007).

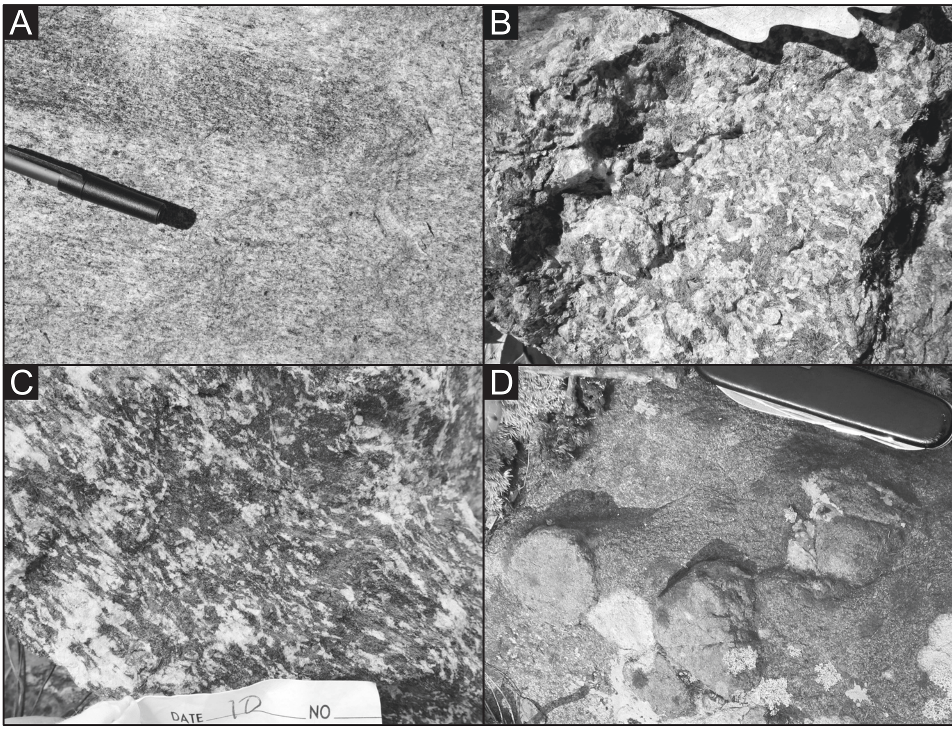

Fig. 4. Field photographs of Cooleyville Gneiss and Packard Gabbro. (A) Typical Cooleyville Gneiss near samples B57 and B57b, with a darker, biotite-rich, deformed inclusion near the top. Sample B57 was dated by Tucker and Robinson (1990, 449 +5/−3 Ma). (B) Coarse-grained Packard Gabbro (sample 4I7), dated by Tucker and Robinson (1990, 407 +3/−2 Ma). (C) Coarse Packard gabbro (sample 10), probably originally much like B, but foliated. (D) Fine-grained, quartz-bearing Packard Gabbro (sample 2F8) with metamorphic garnets 4 cm across, near contact with Partridge Formation a few meters to the east.

GEOCHEMICAL COMPARISONS

Comparison Suite

Two rock units that are similar in geochemistry and age may have similar origins. The geochemistry of the Cooleyville Gneiss and Packard Gabbro have not been previously studied, so one objective was to compare them with regionally important bodies of Paleozoic plutonic rocks. Another reason to have comparative data sets is that the available radiometric ages, one each for the Cooleyville Gneiss and Packard Gabbro, may not be representative of the whole of those bodies. Although the dated Cooleyville Gneiss is lithologically typical, the Packard date is from a very coarse gabbro, unusual for the body on its eastern side (fig. 4B). We therefore make comparisons with plutons similar in age to the two Prescott Peninsula plutonic bodies, and also to two younger, large Devonian plutons that are exposed in the region.

The Cooleyville Gneiss age of 449 Ma is overlapped by the nearby 454 to 442 Ma Monson Gneiss, Fourmile Gneiss, and other parts of the TAPC in the area of figure 2, and the 453 Ma Ammonoosuc Volcanics and 449 Ma Partridge Formation. The 407 Ma Packard Gabbro is about 40 million years younger, and similar in age to parts of the classic New Hampshire Plutonic Suite (NHPS, Lyons and others, 1997; Dorais, 2003), including the Kinsman (403 ± 3 Ma, Lyons and others, 1997) and Spaulding (402 ± 5 Ma, Lyons and Livingston, 1977; 397 ± 1 Ma, Eusden and Barreiro, 1988) sub-types.

Bodies of both sub-types occur extensively in southern New Hampshire (fig. 1). The Coys Hill pluton (fig. 2; 396 ± 2 Ma, Robinson and others, 1982; Morton, ms, 1985; Robinson and Tucker, 1992; no geochemical data available) appears to be connected to the Cardigan pluton of Kinsman (fig. 1), and is mineralogically and texturally like Kinsman.

The Erving Formation (figs. 2 and 3) contains extensive amphibolites, but has no radiometric or fossil age control. However, it appears to overlie the Littleton Formation unconformably (Robinson and others, 1988). The Littleton contains Emsian fossils in northern New Hampshire (Boucot and Arndt, 1960; 407.6–393.3 Ma, Cohen and others, 2013, updated 2018), and U–Pb zircon radiometric ages of ~407 and 407 ± 2 Ma have been determined on felsic volcanics near the base of the Littleton (Rankin and Tucker, 2000). The Erving Formation has been interpreted to immediately underlie the Gile Mountain Formation (Robinson and others, 1988). Fossils in the Gile Mountain and correlative units to the north, in Vermont and Quebec, are also Emsian (Hueber and others, 1990). We conclude that the Erving Formation and its amphibolites are Emsian, similar to the 407 + 3/−2 Ma age of the Packard Gabbro.

The younger plutons we compare to the Cooleyville Gneiss and Packard Gabbro include the Belchertown Complex (380 ± 5 Ma, Ashwal and others, 1979; 381 ± 3 Ma, Tucker and Robinson, 1990), and the Hardwick pluton (360 ± 1, 359 ± 2 Ma; Tucker and Robinson, 1995). Dikes or sills of both of these plutons have been found many kilometers from the main bodies (table A1, Appendix, http://earth.geology.yale.edu/%7eajs/SupplementaryData/2019/Hollocher).

In figures below, we also include for comparison volcanic and plutonic rocks from the Japanese (Honshu) volcanic arc. This is a long-lived, complex volcanic arc that is built on a narrow, rifted segment of Asian continental crust (for example, Taira, 2001). Similarly, the Taconian volcanic arc is also interpreted to have been long-lived, and to have developed on a narrow rifted segment of continental crust.

Silica Variation Diagrams

Figure 5 shows three graphs comparing rocks from the Prescott Peninsula to the other igneous rock data sets. All 29 samples of Packard Gabbro span a range of 48.2 to 53 percent SiO_2, compared to 63.1 to 76.2 percent for the 32 samples of Cooleyville Gneiss, with a gap of nearly 10 percent SiO_2. This gap is consistent with age evidence that these two units are not genetically related.

Rocks from the Hardwick pluton and NHPS Kinsman-type have common intermediate compositions, not found in the Packard Gabbro or Coolyville Gneiss, and tend to have higher aluminum saturation index values (ASI), and Ba and TiO_2 contents. The NHPS Spaulding-type is generally more mafic than the Kinsman and Hardwick, but it also has common intermediate compositions. Rocks of the Belchertown Complex are dominated by intermediate SiO_2 quartz monzodiorites (Ashwal and others, 1979), now recognized as high Ni–Cr–Ba sanukitoids (Robinson and others, 1998; Van Wagner, ms, 2017; see Tatsumi, 2008). The Belchertown also has some Ba-rich mafic rocks (hornblendites), and variable-Ba felsic varieties.

Compositions of the Packard Gabbro and Cooleyville Gneiss overlap those of the Ammonoosuc Volcanics, volcanic layers in the Partridge Formation, and the Monson and Fourmile Gneisses, which have sparse intermediate compositions. The two garnet-rich Packard Gabbro samples have anomalously high ASI values for mafic rocks, probably the result of magmatic assimilation of nearby Partridge Formation schist. Some Ammonoosuc and Partridge volcanic rocks have very low Ba concentrations and high ASI values, possibly the result of chemical alteration (Schumacher, 1988; Hollocher, 1993). Igneous rocks from the Japanese arc also overlap with Taconian plutonic and volcanic rocks, and with samples from the Prescott Peninsula.

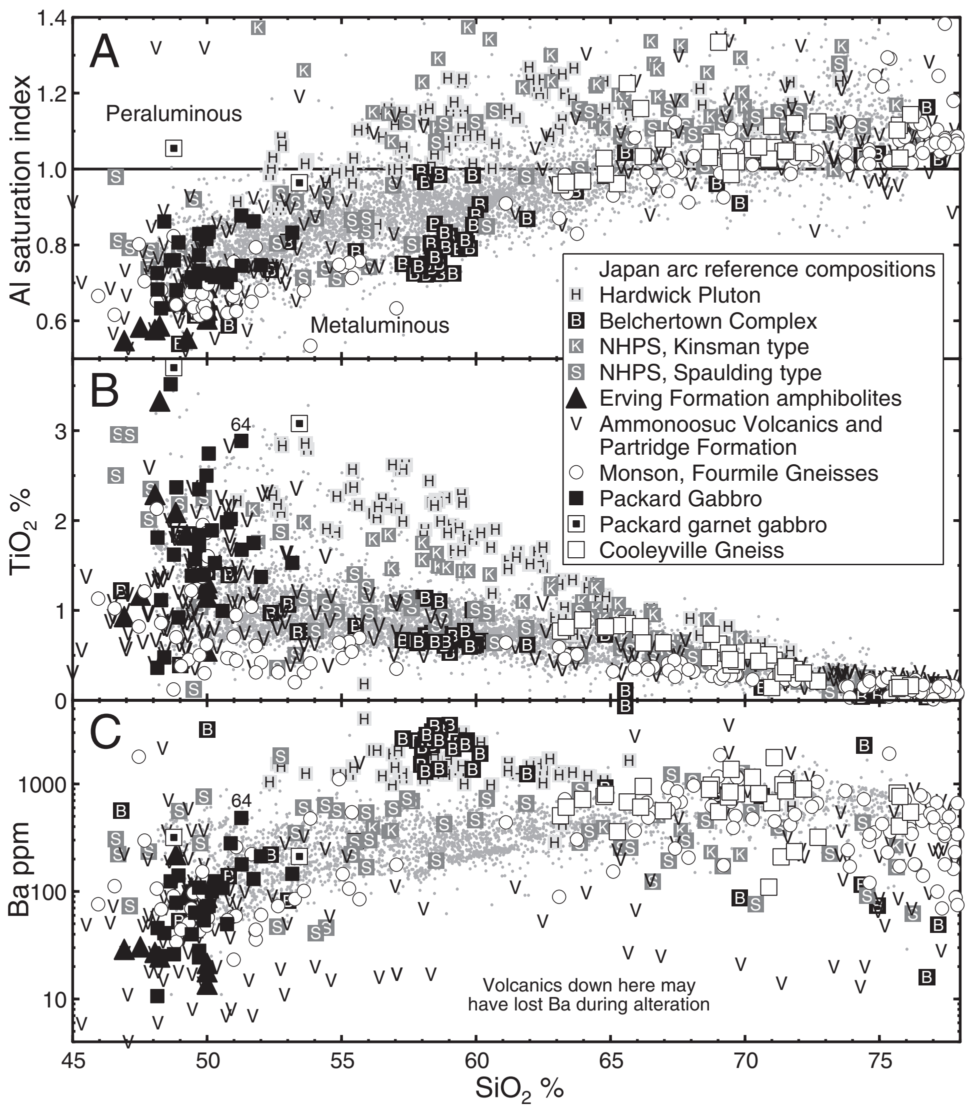

Fig. 5. Silica variation diagrams showing Cooleyville Gneiss, Packard Gabbro, and comparison igneous rock sets. Data for comparison units, except new data in tables A2 and A3 (Appendix), are from Billings and Wilson (1964), Ashwal and others (1979), Leo and others (1984), Tracy and others (1984), Hodgkins (ms, 1985), Hollocher (ms, 1985, 1993), Shearer (ms, 1985), Schumacher (1988), Shearer and Robinson (1988), Leo (1991), Clark and Lyons (1986), Hollocher and others (2002), Dorais (2003), Van Wagner (ms, 2017), apparently unpublished analyses by John Lyons of Spaulding- and Kinsman-types of the New Hampshire Plutonic Suite (five each, written communication from Western Minerals, Inc., Belleair Bluffs, Florida, 1978), and five apparently unpublished Belchertown Complex analyses by Malcom Hill (written communication from Joel Sparks, 1989). Japanese arc reference compositions include about 6500 samples from the GEOROC database, filtered to exclude those noted as being alkaline, not being igneous, having analyzed volatiles >3%, having sums of the 10 major oxides (all Fe as FeO) outside the range of 98–100.5%, SiO_2 contents outside the range of 48.0–76.2%, and older than Cenozoic. Also excluded were samples calculated to be alkaline using the approximate criteria of Ewart (1982, $K_2O > 0.1444 * SiO_2 - 5.1$), and LeBas and others (1986, $K_2O + Na_2O > 0.1765 * SiO_2 - 4.1765$). Aluminum saturation index (ASI): molar Al / (2 * Ca - 3.33* P + Na + K).

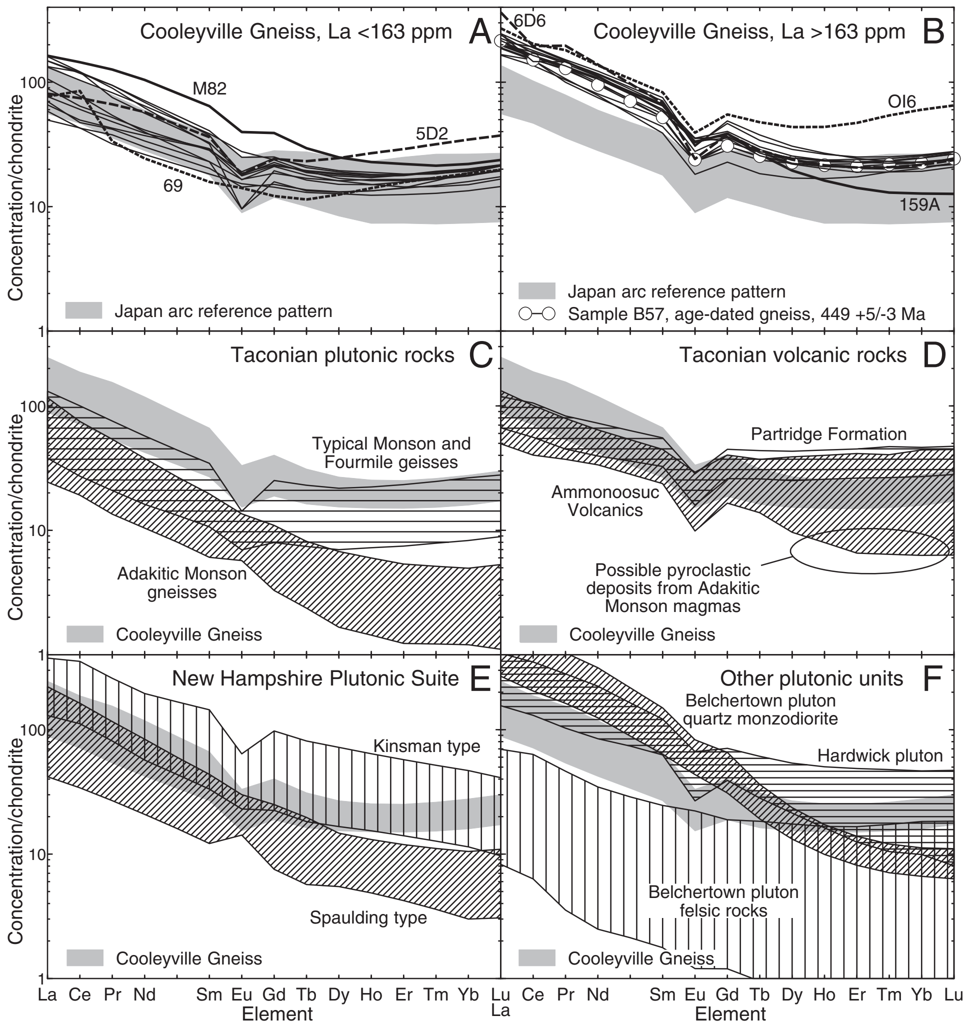

Fig. 6. REE patterns for samples of Cooleyville Gneiss (A, B), and comparison units described in the text (C–F). Data sources are in figure 5. The Japanese arc reference pattern is a subset of that described in figure 5, additionally filtered to have reasonably complete REE analyses, analyses of Zr or Hf, and Nb or Ta, and were restricted to SiO_2 concentration ranges of 63.0–76.2% SiO_2 (here and fig. 8, 228 samples) or 48.0–53.5% (figs. 7 and 9, 760 samples). Fields are averages, ±1 σ, not ranges. Normalizing factors are from McDonough and Sun (1995).

REE Diagrams

Figure 6 shows REE diagrams for the Cooleyville Gneiss and comparison data sets. The Cooleyville Gneiss (figs. 6A and 6B) has La_n/Yb_n ratios of 2.3 to 17, most samples have negative Eu anomalies, all but one (5D2) have concave-upward HREE patterns, and a few have positive or negative Ce anomalies. Such pattern shapes are typical of felsic rocks in volcanic arcs that are built on continental crust, illustrated by the Japanese arc reference pattern. Figure 6C shows that the Cooleyville Gneiss has REE patterns similar to typical Monson and Fourmile gneisses, but not to relatively rare adakitic Monson rocks, which have low HREE concentrations and other compositional characteristics indicative of garnet presence during magma genesis (for example, Defant and Drummond, 1990; Castillo, 2006; Zellmer and others, 2012). REE patterns for felsic rocks in the Partridge Formation and Ammonoosuc Volcanics are somewhat flatter than those of the Cooleyville Gneiss (fig. 6D). Some felsic Ammonoosuc rocks have low HREE concentrations, possibly representing pyroclastic deposits from eruption of Monson adakitic magmas along the arc axis.

Figure 6E shows REE patterns for NHPS Kinsman- and Spaulding-type rocks. These have straighter patterns than the Cooleyville Gneiss, more like adakitic Monson Gneiss in terms of pattern shapes, though the Kinsman has higher REE abundances. The upper edge of the Hardwick Pluton pattern (fig. 6F) approximately parallels the Cooleyville Gneiss pattern, but low HREE values along the Hardwick pattern lower edge indicates the presence of more adakitic, HREE-depleted compositions. Belchertown quartz monzodiorites are strongly LREE-enriched and HREE-depleted compared to the Cooleyville Gneiss. Most Belchertown felsic rocks have much lower REE concentrations than the Cooleyville, though the most REE-rich varieties have similar pattern shapes.

The Packard Gabbro has REE patterns (figs. 7A and 7B) that are less LREE-enriched than the Cooleyville Gneiss (figs. 6A and 6B), with La_n/Yb_n values of 1.5 to 4.6. Those in the lower part of that range (fig. 6A) tend to have slightly concave-downward LREE patterns, compared to straighter patterns in the upper part (fig. 6B). That pattern shape is nearly identical to pattern shapes seen in the Japanese arc, though the Packard Gabbro has average REE concentrations about twice as high. Coarse-grained samples 6A and 6B (fig. 6A) have large, positive Eu anomalies, indicative of cumulus plagioclase. They also have the highest Ni contents among the 29 gabbros, among the highest concentrations of other compatible elements (Mg, Cr, Co), and among the lowest concentrations of REEs, U, and other incompatible elements, characteristics consistent with cumulus origin. Three gabbros have anomalously high REE concentrations (fig. 6B). These include the two quartz- and garnet-rich gabbros that probably have an important schist contamination component. The other is sample 64, which has among the highest concentrations of REEs, U, and other incompatible elements, and Fe, and among the lowest compatible element concentrations (Mg, Cr, Co, Ni). On that basis we suggest sample 64 represents the most strongly fractionated mafic magma.

Packard Gabbro REE pattern shapes are similar to those of typical amphibolites in the Monson and Fourmile gneisses (fig. 7C), but not to rare Nb-rich Monson amphibolites. Ammonoosuc Volcanic and Partridge Formation samples have somewhat flatter patterns than the Packard Gabbro (fig. 7D). Mafic rocks of the NHPS Kinsman- and Spaulding-types (fig. 7E) are more LREE-enriched than the Packard Gabbro. Mafic rocks from the Belchertown pluton, mostly hornblendites, have patterns that overlap those of the Packard Gabbros, though they tend to be flatter (fig. 7F). Amphibolites in the Erving Formation are all LREE-depleted, like N-MORB (for example, McDonough and Sun, 1995), and some Packard Gabbros (fig. 7A).

Multi-Element Diagrams

Figure 8 shows multi-element patterns for the Cooleyville Gneiss and felsic comparative rock sets. All Cooleyville Gneiss samples have negative anomalies for Ti and Nb' (Nb' defined in fig. 8), and positive Th anomalies. Most have large positive Li and Pb anomalies, and variable but mostly negative Sr anomalies. These anomalies, and anomaly sizes, are shared with the Japanese arc reference pattern, and are characteristic of felsic igneous rocks from volcanic arcs (for example, Pearce and Stern, 2006; Yaliniz, 2008). Adakitic Monson gneisses (fig. 8C) have positive Sr anomalies, expected of adakites. Anomalies in the Ammonoosuc Volcanics and Partridge Formation (fig. 8D are similar to those of the Cooleyville, though Li data are lacking. To the extent that data are available (fig. 8E), the NHPS Kinsman-type has

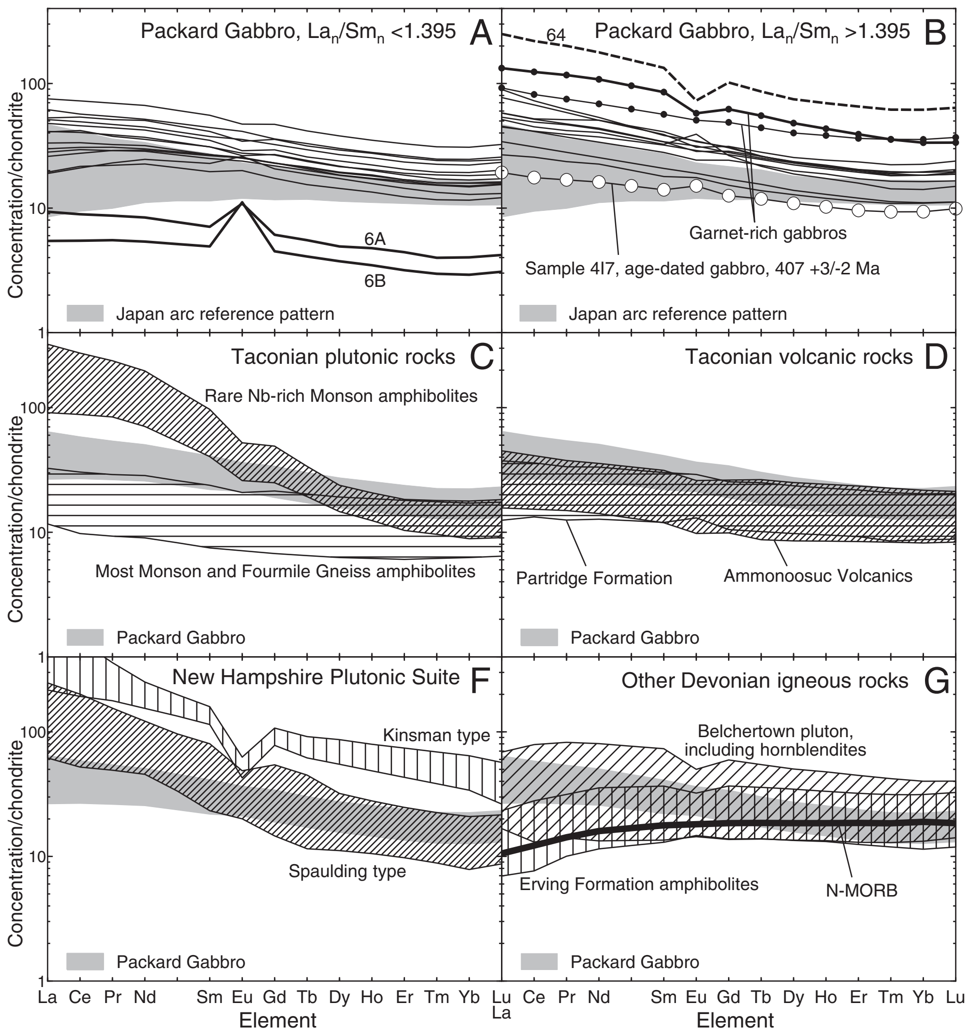

Fig. 7. REE patterns for samples of Packard Gabbro (A, B), and comparison units described in the text (C–F). Data sources are described in figure 5. The Japanese arc reference pattern is as described in figure 6, but including only mafic rocks (760 analyses). Fields are averages, $\pm 1\ \sigma$, not ranges. Normalizing factors are from McDonough and Sun (1995). N-MORB reference pattern is from Sun and McDonough (1989).

anomalies like those in the Cooleyville, but the Spaulding-type has a positive Sr anomaly, unlike the Cooleyville Gneiss, but also seen in the adakitic Monson Gneiss. In figure 8F, the Hardwick pluton has anomalies like those in the Cooleyville Gneiss, as do most of the Belchertown quartz monzodiorites and felsic rocks. However, the quartz monzodiorites tend not to have negative Sr anomalies, like the NHPS Spaulding-type and adakitic Monson Gneiss.

Figures 9A and 9B show multi-element diagrams for the Packard Gabbro and mafic comparison rock sets. All Packard Gabbro samples have positive, generally large Pb and Li anomalies, all but one have negative Nb' anomalies (C01, $Nb'_n/La_n = 1.08$, Nb' and normalization defined in fig. 8) that are generally smaller ($Nb'_n/La_n = 0.35 \pm 0.17$, 1σ) than those of the Cooleyville gneiss (0.53 ± 0.18, 1σ), and all but six have

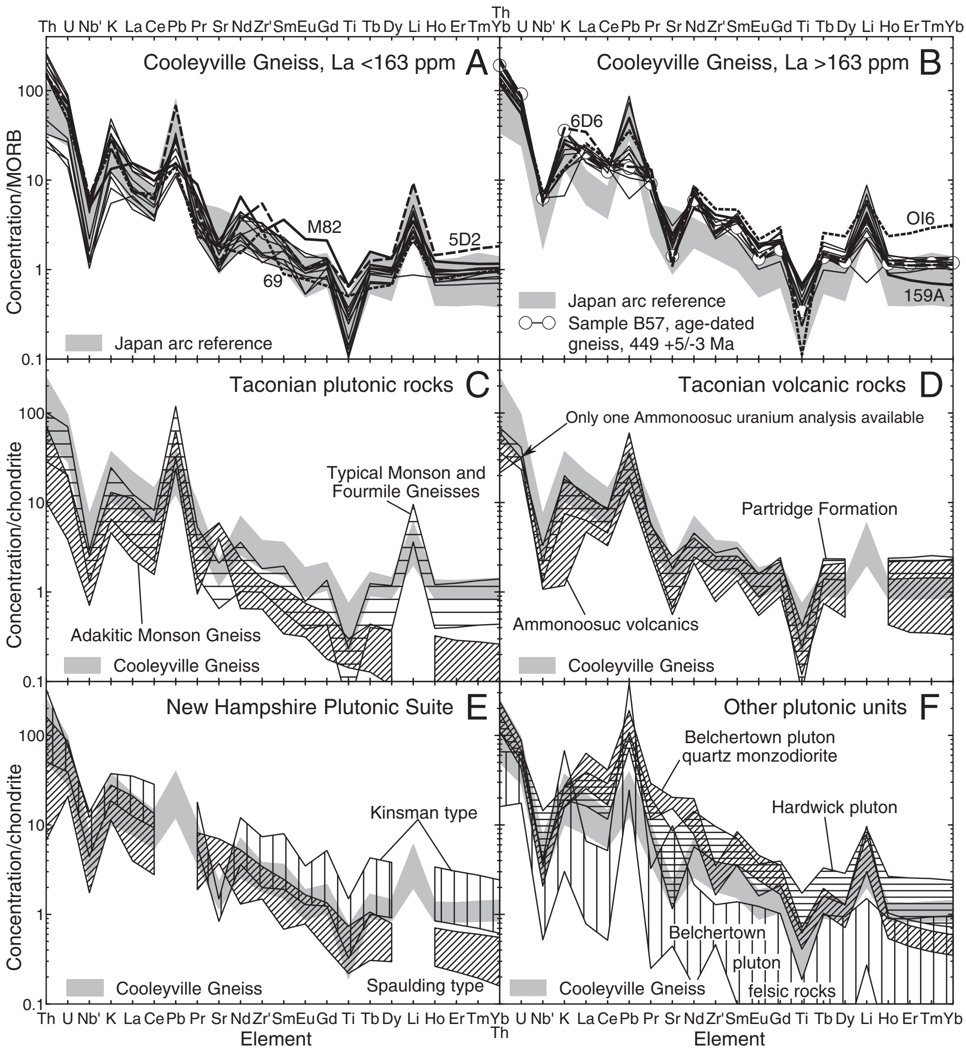

Fig. 8. Multi-element patterns for Cooleyville Gneiss (A, B), and comparison units described in the text (C–F). Data sources are in figure 5. The Japanese arc reference pattern is as described in figure 6, but includes only felsic rocks (228 analyses). Fields are averages, ±1 σ, not ranges. Nb' is MORB-normalized Nb (that is, Nb_n), if data were available, or alternatively normalized Ta. Zr' is MORB-normalized Zr, if data were available, or alternatively normalized Hf. Normalizing factors are from Pearce and Parkinson (1993).

positive Th anomalies ($Th_n/La_n = 2.3 \pm 1.3$, 1σ), also generally smaller than those in the Cooleyville Gneiss (10.6 ± 5.3, 1σ). Anomalies in the Japanese arc reference pattern are similar to those of the Packard Gabbro (figs. 9A and 9B). Samples 6A and 6B have large, positive Sr anomalies, consistent with their likely cumulus origin. Other anomalies are variable and generally small (K, Sr, Zr', Ti). The anomalies seen in Packard Gabbro patterns are consistent with an arc-related environment, as with the Cooleyville Gneiss. Anomalies in the comparison data sets (figs. 9C–9F), including the Erving Formation, are similar to those of the Packard Gabbro, to the extent that data are available. One exception is that the mafic rock pattern from the NHPS Kinsman-type (fig. 9E) has a large, negative Sr anomaly, not seen in the other mafic rock data

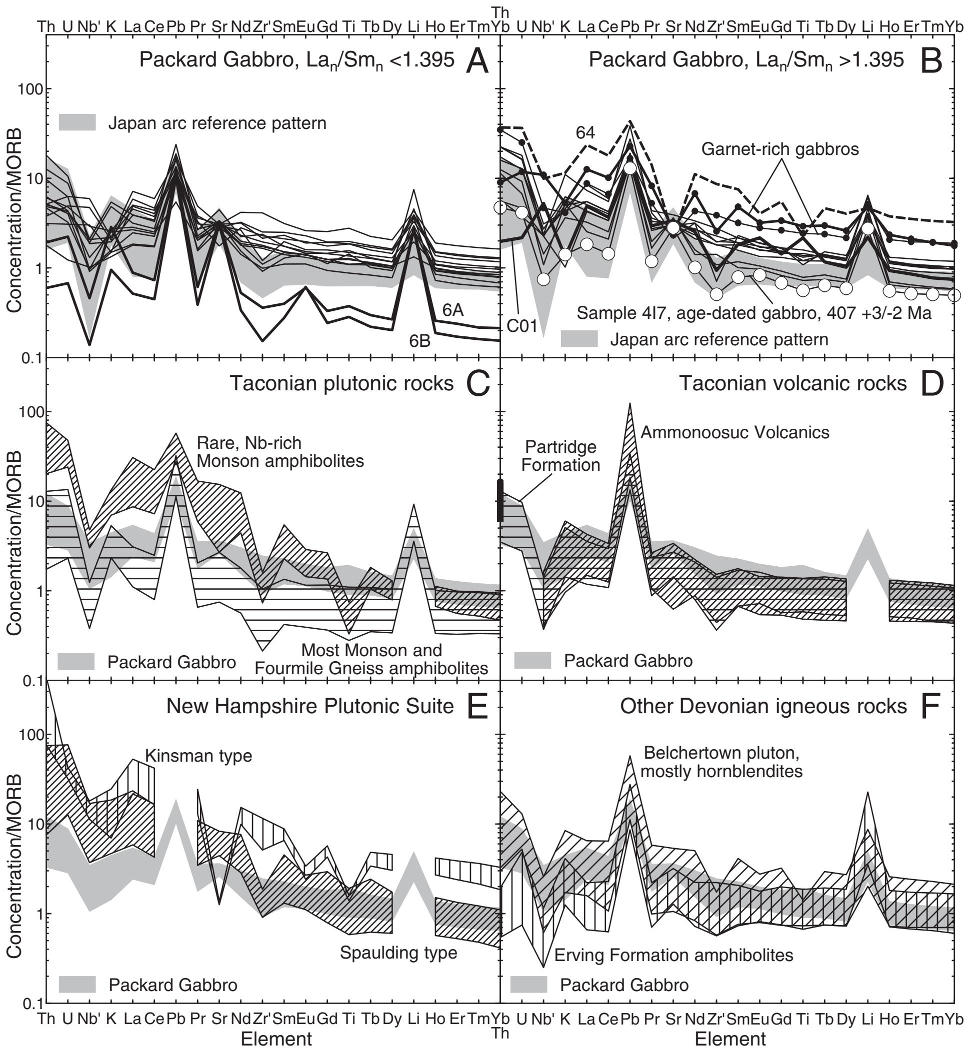

Fig. 9. Multi-element patterns for Packard Gabbro (A, B), and comparison units described in the text (C–F). Data sources are in figure 5. The Japanese arc reference pattern is described in figure 6, but includes only mafic rocks (760 analyses). Fields are averages, ±1 σ, not ranges. Nb' and Zr' are defined in figure 8. Normalizing factors are from Pearce and Parkinson (1993).

sets. Mafic NHPS Kinsman type rocks tend to be biotite-rich and feldspar-poor, rather than hornblende- and feldspar-rich for the others, which may explain the difference.

DISCUSSION

Geochemical Comparison Summary

Figure 5 indicates that Devonian plutonic units in the Central Maine Belt of southern New England (fig. 1), east of the Bronson Hill Anticlinorium (Hardwick, Kinsman, Spaulding), tend to have abundant compositions with intermediate SiO_2, tend to be peraluminous (except mafic rocks), and to have high Ba and Ti concentrations, unlike the Cooleyville Gneiss or Packard Gabbro. The Hardwick, Kinsman, and

Spaulding also tend to have high La_n/Yb_n ratios compared to the Cooleyville Gneiss and Packard Gabbro (figs. 6 and 7). The Belchertown Complex is dominated by intermediate SiO_2 quartz monzodiorites, unlike anything on the Prescott Peninsula, and they and felsic Belchertown varieties have REE patterns and/or concentrations that tend to be quite different than the Cooleyville Gneiss.

The rock sets that have compositions most similar to the Packard Gabbro and Cooleyville Gneiss are the typical Fourmile and Monson Gneisses of the TAPC. Based on age and nearly identical geochemical and lithologic characteristics, we assign the Cooleyville Gneiss to the TAPC, joining the Monson and Fourmile Gneisses. We also conclude that both of the dated Cooleyville Gneiss and Packard Gabbro samples have compositions consistent with the rest of those units, and so are unrelated to the other Devonian plutons in the comparison rock sets.

One striking similarity between all the plotted rock sets is that they have multi-element patterns that imply an arc relationship (figs. 8 and 9). This relationship may have involved: 1) production of the magmas by normal arc processes above a once-active subduction zone (as is interpreted for all Taconian igneous rocks), 2) inheritance from melting of deep crustal rocks that themselves were derived from arc sources (felsic rocks only, peraluminous if melting sources were pelitic), and 3) inheritance from melting of mantle previously modified by subduction zone processes (mafic rocks only, unless strongly modified by processes in the crust prior to emplacement).

Contact Between the TAPC and Stratified Units

The units in contact with the Monson and Fourmile gneisses, and related rocks to the north and south, differ from place to place (fig. 2). In some places, particularly in eastern and southern parts of the Pelham Dome, the Early Silurian Clough Quartzite and Early Devonian Littleton and Erving Formations unconformably overlie the TAPC. More extensively the contact is overlain by the Ordovician Partridge Formation or Ammonoosuc Volcanics. The contact between the TAPC and the Ammonoosuc and Partridge has been controversial, variously interpreted as: 1) An unconformity (Robinson, 1979; Schumacher, 1988), based in part on lack of crosscutting relationships and the thin, locally exposed Moosehorn Conglomerate (Oamc, fig. 3) on the contact at the base of the Ammonoosuc Volcanics. Reexamination of this outcrop in 2017 (Robinson and Hollocher, and Peter Thompson) led to doubts that the unit was a conglomerate at all, that it might instead be a fault breccia. 2) An intrusive contact (most prominently by Leo and others, 1984; Leo, 1985, 1991), based on geochemical and structural interpretations, mostly in west-central New Hampshire. 3) A fault (intra-arc detachment, Tucker and Robinson, 1990; Robinson and Tucker, 1996; Robinson and others, 1998; syn- or post-metamorphic thrust, Kohn and Spear, 1999).

Robinson and his students (for example, Michener, ms, 1983; Schumacher, 1988; Peterson, ms, 1992) found no evidence that the Monson Gneiss, Fourmile Gneiss, or other nearby rocks of the TAPC (fig. 2) intrude the Ammonoosuc Volcanics or Partridge Formation along contacts in Massachusetts and southwestern New Hampshire. The age overlap of gneisses and volcanics, locally and in New Hampshire where ages of the TAPC and Ammonoosuc Volcanics extend to older ages (see age compilations in Hollocher and others, 2016; Karabinos and others, 2017), the apparent lack of intrusive relationships in many areas, the remarkably continuous internal stratigraphy in parts of the Ammonoosuc Volcanics, and the fact that both the Partridge and Ammonoosuc are each in contact with the underlying gneisses in different areas, imply that the contact at the top of the TAPC is a highly-deformed, metamorphosed fault in most places (Robinson and others, 2017).

Cooleyville Gneiss Intrusive Emplacement and Fault Model

The Cooleyville Gneiss clearly intrudes the adjacent Partridge Formation and Ammonoosuc Volcanics (Makower, ms, 1964; fig. 3), but the TAPC gneisses in the area of figure 2 and elsewhere apparently do not, as discussed above. The Partridge Formation and Ammonoosuc volcanics, in different areas, are both in sharp, planar contact with the underlying Monson and Fourmile Gneisses. This contact is interpreted here as a major low-angle detachment fault. If correct, then presumably the Ammonoosuc and Partridge were originally deposited off the arc axis in either the fore-arc (west) or back-arc (east) regions. Hollocher (1993) and Hollocher and others (2002) argued that the Partridge and Ammonoosuc formed in the Taconian back-arc, east of the Bronson Hill belt. In favor of back-arc origin is that, to our knowledge, no boninites have been found in the Ammonoosuc Volcanics or Partridge Formation. Boninites would imply a forearc origin (for example, Reagan and others, 2010; Whattam and Stern, 2011). However, boninites have been found in the Taconian forearc in Charlemont, Massachusetts (fig. 1; Kim and Jacobi, 1996), west of the Bronson Hill Anticlinorium.

Detachment faults are common in volcanic arcs, where they may be associated with subduction initiation, back-arc rifting, and lateral relaxation of collisional belts. Detachment faulting moves shallow-level rocks downward to expose deeper levels, producing structures that, in some cases, have been termed metamorphic core complexes (for example, Brown and others, 2016). Here we give some examples from outside of New England.

Recent initiation of subduction beneath southern Mindanao, Philippines, has produced the young Cotobato Trench (Hall, 2018). Detachment faulting of the southern Mindanao margin has transported Luzon arc volcanics in the hanging wall, produced by subduction on the east side of Mindanao, down and southwest toward the new trench. Another example is in the southern Sierra Nevada batholith, the plutonic roots of a Mesozoic arc built on the western Laurentian margin. Chapman and others (2012) described a large-scale detachment fault that cuts a Cretaceous part of the batholith, moving the hanging wall down and southwestward tens of kilometers, toward or oblique to the subduction zone, involving 5 to 10 km of crustal section. Based on rapid cooling, estimated using U/Pb, Ar/Ar, and U–Th/He dating, faulting took place soon after cessation of arc magmatism.

Collisional orogens also experience detachment faulting as part of the slab detachment, lateral relaxation, and exhumation processes. The coastal hinterland of the Scandinavian Caledonides has an extensive detachment fault system that developed late in the Scandian collision (Silurian–early Devonian), allowing the formation of large Devonian extensional sedimentary basins, and exhuming structural uplifts of deeper levels (for example, Braathen and others, 2000; Osmundsen and others, 2006; Vetti and Fossen, 2012). Lastly, in central Cuba, post-collisional detachment faulting was partly responsible for unroofing the Late Cretaceous–Paleogene Escambray Complex, including the adjacent Trinidad and Sancti Spiritus Domes (Despaigne-Díaz and others, 2016). The originally foreland-dipping detachments are geometrically very similar to those we infer for the Taconian arc.

Figure 10 shows a scenario for movement of the Partridge Formation, Ammonoosuc Volcanics, and Cooleyville Gneiss, from east of the Taconian arc axis, down and west onto the Taconian plutonic complex. In this concept, the Cooleyville Gneiss intruded the Partridge Formation and Ammonoosuc Volcanics on the eastern arc margin (fig. 10A). Following arc collision with Laurentia and during subducted slab foundering, intra-arc extensional collapse along the Moosehorn Fault decapitated the Cooleyville Pluton, moving it and adjacent units down and westward (fig. 10B). A second detachment, the Stoneville Fault, allowed the Partridge Formation and Ammo-

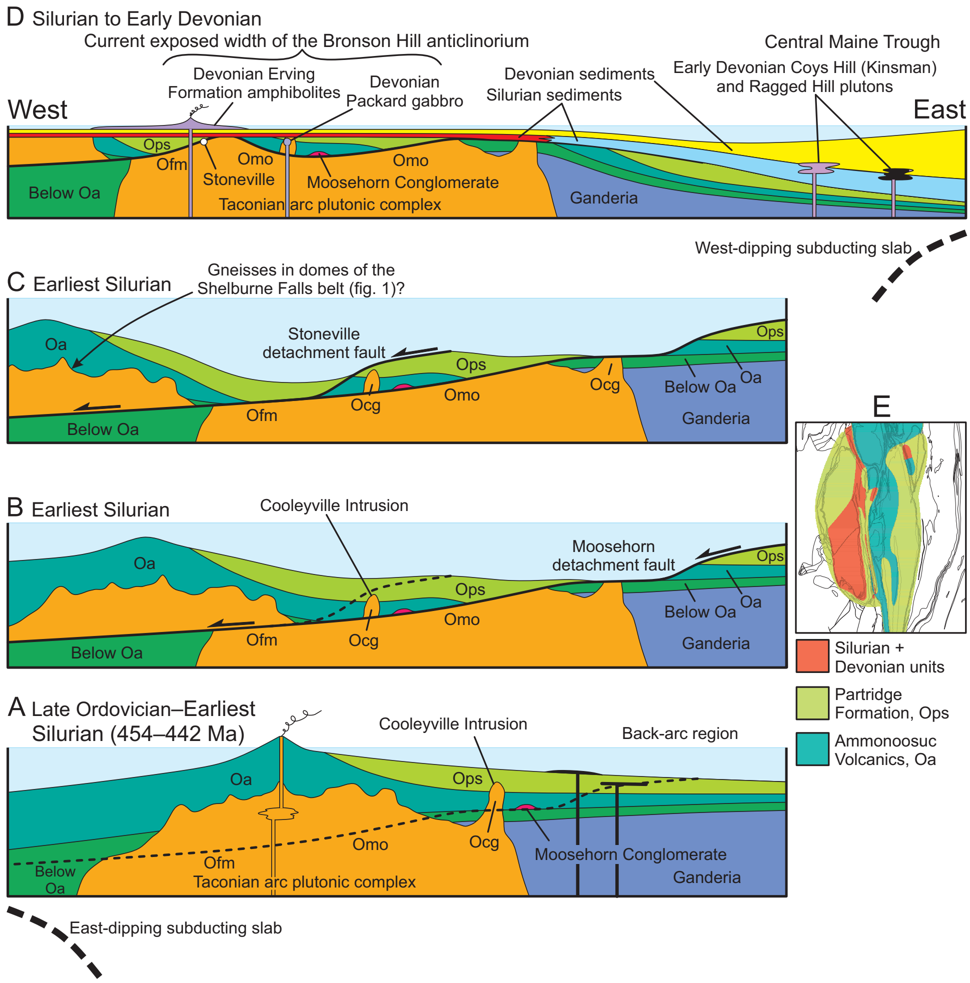

Fig. 10. Model for development of Central Massachusetts, from just prior to the Ordovician Taconian collision with Laurentia to emplacement of the Packard Gabbro, early in the Devonian Acadian Orogeny. (A) Active Taconian arc just prior to collision, with emplacement of the youngest arc magmas. (B, C) Post-collisional collapse of the Taconian arc along detachment faults during subducted slab foundering and arc extension. (D) Isostatic relaxation and erosion, with slow lithospheric cooling permitting subsidence and Silurian and Devonian sedimentation. New igneous activity is related to subduction of Iapetan ocean crust westward beneath the Central Maine Belt, as Avalon approached composite Laurentia, emplacing early parts of the New Hampshire Plutonic Suite, the Packard Gabbro, and Erving Formation volcanics. Unit colors in A–D are from figure 2. (E) Units in contact with the Taconian arc plutonic complex, above the inferred detachment faults (Ammonoosuc Volcanics and Partridge Formation) or above unconformities (Silurian and Devonian units, abstracted from fig. 2).

noosuc Volcanics to slide into their current relative positions. In this model, mostly Partridge Formation is in contact with the TAPC to the west and east, with a belt of mostly Ammonoosuc Volcanics in between (fig. 10C). Later isostatic readjustment, erosion, and cooling allowed deposition of Silurian and Devonian sediments, in unconformable contact with the underlying Ordovician units (fig. 10D), as is currently seen in the map pattern (figs. 2 and 10E). Although other fault geometries can yield similar results, the proposed model is the simplest of those we have considered.

In western New Hampshire, there is clear evidence that the Ammonoosuc Volcanics and Partridge Formation are cut by Taconian-age intrusives in some places, along or west of the central axis of the Bronson Hill anticlinorium. These intrusive bodies include the Chickwolnepy intrusions (Aleinikoff and Moench, 1987, 1992; Fitz, 2002; Moench and Aleinikoff, 2003; Aleinikoff and others, 2015), the Joslin Turn pluton (Aleinikoff and Moench, 1992; Rankin and others, 2013), the Plainfield Tonalite (Valley and Walsh, 2013; Valley and others, 2015), and parts of the Lebanon and Sugar River domes (Valley and Walsh, 2013; Valley and others, 2015). However, in most places the planar, non-intrusive contact we describe in Massachusetts and southwestern New Hampshire, at the top of the TAPC, appears to continue into north-central New Hampshire (Lyons and others, 1997).

In the Bronson Hill Anticlinorium of north-central New Hampshire, Eusden and others (2006, 2017) reported that the Ammonoosuc Volcanics is in contact with underlying Ordovician gneisses on the southeastern flank of the Jefferson Dome, along the Moose River Fault. Late shear sense indicators on the east-dipping fault surface indicate late normal motion, interpreted to represent Devonian (Acadian) deformation. However, early motion sense indicators were reported to indicate reverse fault motion, which may have been normal (tops down to the west) detachment motion prior to Devonian deformation. We suggest that early motion on this fault represents post-Taconian collision detachment faulting such as we describe to the south.

In Connecticut, the TAPC includes extensive exposures in the Glastonbury Dome (fig. 1), and an extension of the Monson Dome in Massachusetts that ultimately connects to the Killingworth Dome. In that region, TAPC rocks appear to be in planar contact with the Ordovician Middletown and Collins Hill Formations (Rodgers, 1985; Ammonoosuc Volcanics and Partridge Formation equivalents), in different areas, such as we describe in Massachusetts. The Silurian Clough Quartzite and Devonian Littleton Formation are in unconformable contact with the TAPC in Connecticut in some places, also as seen in Massachusetts.

In this model, post-Taconian detachment faults have placed Ordovician and possibly older stratified rocks (Albee Formation, Rankin and others, 2013) into contact with the underlying TAPC along most of the Bronson Hill Anticlinorium. Taconian-age intrusions into stratified rocks, as described above, we interpret to be either decapitated intrusions in the detachment fault upper plate, now exposed close to or west of the Bronson Hill–TAPC axis, or autochthonous parts of the TAPC intrusions from below the detachment surfaces.

Based on evidence in Massachusetts and southwestern New Hampshire, detachment fault movement must have occurred between the ages of the youngest Monson Gneiss (442 $+ 3/-2$ Ma, Tucker and Robinson, 1990), and the unconformably overlying Silurian Clough Quartzite (Telychian, ~438.5–433.4 Ma, Cohen and others, 2013, updated 2018; on the basis of fossils in the Clough in New Hampshire, Boucot and Thompson, 1958, 1963; Boucot and others, 1958), an interval of not more than ~6.5 ± 5 million years.

Packard Gabbro Emplacement

The 407 Ma Packard Gabbro (Tucker and Robinson, 1990) appears to be geochemically similar to typical amphibolites in the much older Monson and Fourmile Gneisses, rather than coeval or younger Devonian plutons in southern New England. As discussed above, the gabbro is approximately the same age as amphibolites in the Early Devonian (Emsian) Erving Formation. The Erving and Packard also have almost identical multi-element anomalies that are indicative of arcs. We conclude that these two mafic units probably represent magmas from the same igneous episode. However, all Erving Formation amphibolites analyzed so far have N-MORB-like, LREE-depleted

REE patterns (fig. 7G). A few Packard samples have similar REE patterns and concentrations, but most are somewhat LREE-enriched. Although some Packard Gabbros are likely cumulates, based on geochemical indicators and coarse texture (for example, samples 6A, 6B, figs. 4B and 4C, discussed above), most are not. If most gabbros approximately represent magma compositions, then the different REE patterns in the two units need explanation.

We suggest that Devonian subduction beneath the Central Maine Belt (fig. 10D), early in the Acadian Orogeny (for example, Watts and others, 2000), induced minor melting in remnant Taconian lithospheric mantle under the Bronson Hill region. The location of Packard Gabbro emplacement, considerably west of the main belt of southern New England Devonian plutonism, suggests that this melting was related to distant, limited, possibly back-arc processes. The rising of small volumes of mafic magma, through Taconian shallow mantle and crust, led to eruption of mafic volcanics of the Erving Formation and emplacement of the Packard Gabbro (possibly also the Mt. Hermon Gabbro, fig. 2). The fact that the Erving and Packard are not compositionally identical may indicate that the two are not part of the same magmatic plumbing system. Instead, we infer that the remnant Taconian mantle was inhomogeneous on a scale of several (tens of?) kilometers, leading to somewhat different magma compositions in the two units.

During emplacement of small volumes of mafic magma into the Bronson Hill region, more voluminous intermediate and felsic magmatism was occurring farther to the east and northeast, producing older parts of the NHPS. In those areas, subduction zone magmas interacted with the thick sedimentary section in the Central Maine Belt, leading to petrologically and geochemically very different igneous rocks exposed at the present surface.

CONCLUSIONS

The Prescott Peninsula contains two intrusive bodies, the 449 Ma Cooleyville Gneiss, and the 407 Ma Packard Gabbro. The Cooleyville was probably emplaced as a series of small, shallow Taconian arc intrusions into the Partridge Formation and Ammonoosuc Volcanics, east of the arc axis, currently exposed as the TAPC of the Bronson Hill anticlinorium. Following collision of the Taconian arc with Laurentia, and during subducted slab foundering and lateral spreading of the orogen, movement along the Moosehorn detachment fault decapitated the plutonic precursor to the Cooleyville Gneiss, sliding it and host stratified units west and down into contact with the TAPC along the extinct arc axis. A second, Stoneville detachment fault put the Partridge Formation in contact with the TAPC farther west. This placed the Partridge Formation in contact with the TAPC on both the east and west sides of this part of the Bronson Hill Anticlinorium, with Ammonoosuc Volcanics along the contact in the center. Following isostatic readjustment, erosion, and cooling, the Silurian Clough Quartzite and Devonian Littleton Formation were unconformably deposited on the older rocks. This model suggests that metamorphosed Ordovician arc plutonic and volcanic rocks in the Shelburne Falls Belt (fig. 1), may be the transported upper parts of the same arc complex presently exposed in the Bronson Hill anticlinorium.

Renewed Devonian mafic igneous activity in the Bronson Hill region coincided with voluminous, mostly intermediate and felsic Early Devonian NHPS plutonism in the Central Maine Belt, east of the Bronson Hill Anticlinorium. In the Bronson Hill region, Devonian igneous activity may have involved melting of remnant Taconian arc lithospheric mantle, reactivated by Acadian subduction. Mantle melting resulted in emplacement of the 407 Ma Packard Gabbro, and eruption of mafic volcanics of the Emsian Erving Formation. Those magmas passed relatively unchanged through remnants of the Taconian shallow mantle and igneous crust. Following complex Acadian and later metamorphism, Mesozoic brittle faulting on the west and north margins of the Cooleyville Gneiss offset it and the Packard Gabbro down and southeastward. This movement juxtaposed the Ordovician Cooleyville Gneiss against Silurian Clough Quartzite and Devonian Littleton Formation in the Prescott Syncline.

Work needed to test and extend our ideas includes additional geochemistry on the Erving Formation amphibolites to better understand their compositional range, additional radiometric dating constraints on the Cooleyville Gneiss, Packard Gabbro, and local TAPC gneisses, and geochemical and geochronological work on the Mt. Hermon Gabbro, a possibly related intrusion.

Numerical modeling of detachment fault development in the Aegean Sea back-arc region (Huet and others, 2011) indicates that successive detachment faults in an evolving metamorphic core complex can result in multiple structural domes in the same system (see also Rey and others, 2011). The belt of parallel and staggered structural domes in the Bronson Hill anticlinorium (figs. 1 and 2) may have had their pre-Devonian start as low-amplitude structures related to post-Taconian development of multiple, in part overlapping detachment faults. The concept of intra-arc and post-collision detachment faulting is not new, but evidence for it can be obscured by severe regional metamorphism. We hope this example helps with the recognition of similar pre-metamorphic fault systems in other collisional orogens.

ACKNOWLEDGMENTS

We thank the Massachusetts Geological Survey for funding analytical work, and several University of Massachusetts graduate students for help with sample collection. We thank the Massachusetts Department of Conservation and Recreation for providing the permit for sampling within the Quabbin Reservoir Reservation. We appreciate the helpful reviews of this manuscript by Michael Dorais and Nick Ratcliffe, three anonymous reviewers, and additional constructive comments from Raymond M. Russo and Mike Williams. We thank the Union College Geology Department for supporting analytical and field work, and the National Science Foundation, grants DUE-9952410 and MRI-1726075, for supporting analytical instrumentation.

APPENDIX

TABLE A1

Description of sample sets in tables A2 and A3.

Sample sets	Descriptions
Prescott Peninsula: Cooleyville Gneiss and Packard Gabbro	Sixty new samples were collected in the spring and summer of 2016, including 29 gabbros and 31 gneisses. Most were collected within the Quabbin Reservoir Reservation, under permit from the Massachusetts Department of Conservation and Recreation. Sample locations are shown on figure 3, samples described in table A2, analyses shown in tables A3-1(*major elements*) and A3-2 (*trace elements*). To this set we added sample B57, a crushed split of the Cooleyville Gneiss sample dated by Tucker and Robinson (1990), analyzed by XRF in 1986 (Hollocher, unpublished). New sample B57b is from the same outcrop.
Fourmile Gneiss	New analyses were done for several Fourmile Gneiss samples that were originally collected and crushed by Jon Bull (in part reported in Bull, 1997; also see Hollocher and others, 2002). These include six amphibolites in the Devonian Erving Formation, two of Fourmile Gneiss that were never analyzed, seven of Fourmile gneiss analyzed for major and some trace-elements by XRF, but not for REE and other trace-elements, and 25 that were analyzed for major and some trace-elements by XRF and for REE, but not other trace-elements. Sample locations are given in table A2, and complete data, including previously published values, are in tables A3-1(*major elements*) and A3-2 (*trace elements*). The samples collected and crushed by Bull were powdered by him in a Spex® tungsten carbide ring mill. Tungsten carbide contamination is the reason those samples were not analyzed for cobalt, molybdenum, or tantalum.
Hardwick Pluton, Belchertown Complex, Erving Formation amphbolite	To expand the data set for regional geochemical comparisons, we analyzed two new samples from the Hardwick pluton (figs. 1, 2; also see Shearer, 1985; Robinson and Tucker, 1992), one biotite tonalite from the pluton interior and one garnet–biotite tonalite from the eastern margin, six samples from the Belchertown Complex (fig. 2; the Three Rivers railroad cut of Ashwal and others, 1979; also see Ashwal, 1974), five quartz monzodiorites and one tonalite dike), and four new samples from the Erving Formation. Sample locations and descriptions are in table A2, and data are in tables A3-1(*major elements*) and A3-2 (*trace elements*).

Dikes or sills of the Belchertown Complex and Hardwick pluton have been found many kilometers from the main bodies (Belchertown: samples N164 and TR25+06 of Hodgkins, 1985 and sample 6 of Tucker and Robinson, 1990; Hardwick: Hollocher, 1993, sample 41, assignment to Hardwick made in 2002). This supports the concern that parts of the Cooleyville Gneiss or Packard Gabbro could be related to these other plutonic bodies.

TABLE A2

Sample locations and descriptions

Sample	Topographic quadrangle	Latitude (°N)[1]	Longitude (°W)[1]	Elev. (m)[1]	Unit	Description
3	Quabbin Reservoir	42.4611	72.35273	395	Packard Gabbro	About three meters southeast of exact summit of Packard Mtn. (hill 1281). Very fine-grained gabbro.
8	Quabbin Reservoir	42.4569	72.35472	286	Packard Gabbro	Relatively coarse gabbro with plagioclase up to 1 cm, most about 3-4 mm. This is a low outcrop, possibly not quite in place, somewhat weathered.
11	Quabbin Reservoir	42.4383	72.36163	254	Packard Gabbro	Fine-grained "Prescott diorite" from a roadside outcrop.
46	Quabbin Reservoir	42.4491	72.35430	339	Packard Gabbro	Fine-grained gabbro between two low crops, 10-15 m away, that have schist inclusions.
64	Quabbin Reservoir	42.4646	72.33565	294	Packard Gabbro	Low outcrop facing the road, numerous flat slabs above and to the the sides of the collecting spot. Fine-grained, hornblende-bearing gneiss.
159	Quabbin Reservoir	42.4512	72.37071	225	Packard Gabbro	Outcrop includes the contact between gneiss to the west and gabbro to the east. Gneiss was badly weathered, and gabbro highly fractured, with lots of white veins, but a good gabbro sample taken.
233	Quabbin Reservoir	42.3945	72.33981	243	Packard Gabbro	Large angular block of gabbro, may not be outcrop but is pretty close.
578	Quabbin Reservoir	42.47270	72.35131	311	Packard Gabbro	Road cut on the north side of Rt. 202. Fine-grained amphibolite, dark, several folded pegmatite veins nearby.
10c	Quabbin Reservoir	42.4428	72.33976	266	Packard Gabbro	Just downhill and toward the road from 2K3. This is a relatively coarse-grained, deformed gabbro with augen up to 1.5 cm.
10f	Quabbin Reservoir	42.4428	72.33976	266	Packard Gabbro	Just downhill and toward the road from 2K3. This is a relatively fine-grained, almost ultramafic hornblende-rich gabbro with augen up to 1 cm.
1I3	Quabbin Reservoir	42.4511	72.35004	315	Packard Gabbro	Large, northeast-facing outcrop of gabbro, medium-grained.
1I6	Quabbin Reservoir	42.4503	72.35229	340	Packard Gabbro	Low, flat outcrop on ridge, very fine-grained gabbro.
2F4	Quabbin Reservoir	42.47935	72.33187	285	Packard Gabbro	One of many sizeable outcrops on this west-facing slope. Medium-grained gabbro with ~5 mm plagioclase in finer-grained matrix of hornboende and plagioclase.
2F6	Quabbin Reservoir	42.47931	72.33092	307	Packard Gabbro	Coarse, almost undeformed gabbro, with pinkish plagioclase. Hornblende is up to 1.5 cm long, though most is about 5 mm. Tall outcrop near northwest edge of logged area.
2F8	Quabbin Reservoir	42.47806	72.33117	255	Packard Gabbro	Sample of garnet gabbro, near road and logging track, low, west-facing outcrop partly covered by logging debris. Sample is from within a few meters of the northeast Packard Gabbro contact with Partridge Formation muscovite schist.
2I1+100m	Quabbin Reservoir	42.4472	72.3554	343	Packard Gabbro	Location is ~100 meters southwest of 2I1a and b, medium-grained gabbro. No GPS reading, so position is interpolated between location 2I1 and another non-sample station about an equal distance in the opposite direction. Elevation is estimated from the walk along the ridge.
2I1a	Quabbin Reservoir	42.4476	72.35562	348	Packard Gabbro	Fine-grained gabbro, one sample from the west end of the outcrop.
2I1b	Quabbin Reservoir	42.44763	72.35562	348	Packard Gabbro	Fine-grained gabbro with pale, ~2 cm garnet lumps, taken about 3 meters north of sample 2I1a. This part of the outcrop was rusty-weathering and biotite-rich, possibly contaminated by nearby, unseen schist xenoliths.
2K3	Quabbin Reservoir	42.4431	72.33929	310	Packard Gabbro	Fine-grained gabbro with large (5 mm) hornblendes that cause the rock to weather with bumps.
2K5	Quabbin Reservoir	42.4425	72.33964	277	Packard Gabbro	Short distance from 10, fine-grained gabbro without lumps. This crop had a thin, pink dikelet, a coarser gabbroic dike, and a garnet-lump layer, probably a partially reacted xenolith of schist.

TABLE A2
(continued)

Sample	Topographic quadrangle	Latitude (°N)[1]	Longitude (°W)[1]	Elev. (m)[1]	Unit	Description
3I7	Quabbin Reservoir	42.438	72.35388	360	Packard Gabbro	Medium-grained gabbro on the southeast side of the summit knob.
3I7A	Quabbin Reservoir	42.4381	72.35476	358	Packard Gabbro	Fine-grained gabbro, just west of station 3I7. This location is on the south side of the hilltop, a few meters below the summit. It is a large field of angular blocks and slabs of the same fine-grained rock.
43A	Quabbin Reservoir	42.4397	72.35069	344	Packard Gabbro	Medium-grained gabbro from the west facing side of the knob, north of where PR site 43 should be.
4D3	Quabbin Reservoir	42.4432	72.36654	210	Packard Gabbro	Low wall facing the road under a huge dead pine tree. This is relatively coarse gabbro.
4I7	Quabbin Reservoir	42.43723	72.34306	308	Packard Gabbro	Very coarse hornblende-plagioclase gabbro with red spots that are probably weathered sulfides. Tucker and Robinson (1990) geochronology sample 13 = PR-88-14
6A	Quabbin Reservoir	42.4535	72.36249	294	Packard Gabbro	Northeast of summit 933, a series of ledges on the slope, and this one is from near the top. Very coarse gabbro with pale gray-green hornblende up to 1.5 cm long, also with some biotite. Plagioclase is relatively fine, and some have tiny red garnets associated with them.
6B	Quabbin Reservoir	42.45240	72.36292	292	Packard Gabbro	Sample is from the south end of the summit of hill 933. The sample is medium-grained with no garnets and black hornblende.
BL	Quabbin Reservoir	42.44	72.34892	332	Packard Gabbro	Fine-grained gabbro on a low ridge that crosses the main ridge. Very fresh and equigranular.
C01	Quabbin Reservoir	42.4607	72.35301	424	Packard Gabbro	Down the ridge to the southwest from the summit. Fine-grained gabbro from a series of low ledges and angular blocks.
6.5	Quabbin Reservoir	42.45222	72.36197	282	Cooleyville Gneiss	This sample location is about half way between PR stations 6 and 7, on hill 933. Outcrop is a northwest-facing wall of medium-grained, very feldspathic Cooleyville Gneiss.
18	Quabbin Reservoir	42.47907	72.35723	329	Cooleyville Gneiss	Hill 1115, a low cluster of angular blocks near the south tip of the knob. Fine-grained gneiss, pretty fresh and brittle.
39	Quabbin Reservoir	42.48362	72.35374	364	Cooleyville Gneiss	Low outcrop and north-facing ledge just north of the summit of hill 1203. Fine-grained gneiss, somewhat weathered with coarser, leucocratic streaks, possibly xenoliths.
40	Quabbin Reservoir	42.48201	72.35121	355	Cooleyville Gneiss	Low cluster of angular slabs in the low point between a low knob to the south and a higher ridge to the north. Fine-grained gneiss that contains nnumerous small biotite-rich xenoliths that could not be avoided.
69	Quabbin Reservoir	42.42187	72.35060	334	Cooleyville Gneiss	Fine-grained Cooleyville Gneiss. From outcrop slabs a little west of the exact hill summit, above transition to steep slope.
74	Quabbin Reservoir	42.42295	72.33418	297	Cooleyville Gneiss	Roughly 130' from B57, and looks just like it. Fresh gneiss, biotite, magnetite, fine-grained, deformed.
75	Quabbin Reservoir	42.42369	72.33563	323	Cooleyville Gneiss	Fresh gneiss, biotite, magnetite, fine-grained, deformed, less magnetite than B57
362	Quabbin Reservoir	42.40717	72.34761	323	Cooleyville Gneiss	Hillslope of large, angular slabs, probably within a few meters of outcrop. Medium-grained.
729	Winsor Dam	42.34582	72.32905	272	Cooleyville Gneiss	Somewhat foliated gneiss, possibly muscovite-bearing, with Partridge Formation a little to the east.
747	Winsor Dam	42.33671	72.32610	162	Cooleyville Gneiss	Southernmost exposure of the Cooleyville Gneiss. Sample was from the east side of the stream, east of the pyroclastic-looking, garnet-bearing felsic Ammonoosuc Volcanics, just where you can look north along the lake shore. Biotite gneiss, little foliated.
5E3	Quabbin Reservoir	42.45596	72.33055	306	Cooleyville Gneiss	Low outcrop about 10 m across on west side of Bials Hill, about halfway up the slope. Fine-grained, lineated.

Table A2
(continued)

Sample	Topographic quadrangle	Latitude (°N)[1]	Longitude (°W)[1]	Elev. (m)[1]	Unit	Description
0I6	Quabbin Reservoir	42.42771	72.36456	259	Cooleyville Gneiss	East-facing outcrop on the east side of a knob. Fine-grained, very brittle, garnet-biotite gneiss.
159A	Quabbin Reservoir	42.45078	72.37120	228	Cooleyville Gneiss	Fine-grained gneiss, south and somewhat west of location 159.
4F3	Quabbin Reservoir	42.42453	72.33837	313	Cooleyville Gneiss	Biotite gneiss from a low, sharp, broken, west-facing ledge on the west side of a ridge, facing a new clear-cut area.
4I9A	Quabbin Reservoir	42.43159	72.33336	358	Cooleyville Gneiss	Leucocratic, medium-grained gneiss, slightly orange-weathered, probably a bit east of PR station 4I9, which is on the west side of the ridge.
5D2	Quabbin Reservoir	42.42986	72.33006	328	Cooleyville Gneiss	Coarse gneiss, strongly foliated and lineated, feldspathic, from near-veritcal slabs just east of a swamp, at the southern end of a little ridge.
5IOA	Quabbin Reservoir	42.42975	72.33385	350	Cooleyville Gneiss	This location is southwest of 5IO, where the ridge curves around to face east, more mafic than previous sample, strongly lineated and somewhat orange-weathered throughout.
65a	Quabbin Reservoir	42.42584	72.35502	295	Cooleyville Gneiss	Northwest-facing ledge on a steep slope, sample from the upper-northeastern corner. Medium-grained, hornblende-bearing gneiss.
65b	Quabbin Reservoir	42.42508	72.35520	285	Cooleyville Gneiss	Same outcrop as 65a, but from the southwest end of the outcrop. Biotite but no hornblende.
6D6	Quabbin Reservoir	42.43002	72.33204	332	Cooleyville Gneiss	Gneiss, from large angular slabs that probably slid downhill from a few meters up.
B08	Winsor Dam	42.37027	72.32942	244	Cooleyville Gneiss	Higher ledges of garnet-bearing gneiss.
B10	Winsor Dam	42.37141	72.32891	218	Cooleyville Gneiss	Ledges of gneiss on steep slope on the side of the hill, biotite but no garnet.
B55A	Quabbin Reservoir	42.41610	72.35078	320	Cooleyville Gneiss	Group of long crops along west side of hill. Medium-gray, fine-grained gneiss from near the south end of the outcrop.
B55B	Quabbin Reservoir	42.41610	72.35078	320	Cooleyville Gneiss	Group of long crops along west side of hill. Dark-gray, fine-grained Cooleyville Gneiss from near the middle of the outcrop.
B55Ca	Quabbin Reservoir	42.41610	72.35078	320	Cooleyville Gneiss	Group of long crops along west side of hill. Light-gray, relativley coarse-grained layer in finer-grained, darker Cooleyville Gneiss from near the south end of the outcrop.
B55Cb	Quabbin Reservoir	42.41610	72.35078	320	Cooleyville Gneiss	Group of long crops along west side of hill. Darker-gray, fine-grained gneiss matrix to the leucocratic, coarse-grained layer, from near the south end of the outcrop.
B56	Quabbin Reservoir	42.40390	72.33775	323	Cooleyville Gneiss	Large crop of somewhat layered gneiss, looks like no garnets, quite fresh.
B57	Quabbin Reservoir	42.42320	72.33460	298	Cooleyville Gneiss	Fresh gneiss, biotite, magnetite, fine-grained, deformed. Slightly darker-gray xenoliths. Tucker and Robinson (1990) geochronology sample 12 = PR-88-11.
B57b	Quabbin Reservoir	42.42319	72.33456	298	Cooleyville Gneiss	Same outcrop as B57, but this sample is probably not from exactly the same spot.
KH	Quabbin Reservoir	42.47850	72.34847	293	Cooleyville Gneiss	Low, large outcrop almost within sight of Rt. 202. Relatively light-gray, medium-grained, with small hornblende spots.
M82	Quabbin Reservoir	42.46926	72.36794	226	Cooleyville Gneiss	A series of small outcrops facing and just above the nearby stream. Fine-grained, dark-gray, foliated.

TABLE A2
(continued)

Sample	Topographic quadrangle	Latitude (°N)[1]	Longitude (°W)[1]	Elev. (m)[1]	Unit	Description
M83	Quabbin Reservoir	42.46895	72.36897	238	Cooleyville Gneiss	A series of low ridges next to an overgrown dirt road, very fine-grained gneiss.
JB-06	Unknown	-	-	-	Fourmile Gneiss	Amphibolite, collected and crushed by Bull (1997), but sample not analyzed and location not recorded.
JB-13	Unknown	-	-	-	Fourmile Gneiss	Felsic gneiss, collected and crushed by Bull (1997), but sample not analyzed and location not recorded.
Other samples, Fourmile Gneiss	Several	-	-	-	Fourmile Gneiss	See Bull (1997).
2	Northfield	42.687	72.42484	345	Erving Formation	Low, small outcrops about 15 meters east of the summit of Round Hill. Rock is dark-gray, fine- and even-grained, and quite fresh.
5	Northfield	42.6742	72.42580	296	Erving Formation	Fresh, slabby but homogeneous, fine-grained, dark-gray amphibolite. Taken from a blasted roadcut along Gulf Rd., from about 1/5 of the way along the outcrop from its downhill (northwestern) end.
7	Northfield	42.6554	72.41671	383	Erving Formation	Dark-gray, fine-grained amphibolite, taken from the north end, top part of a small road cut on the west side of Gulf Rd. The amphibolite is layered, but only massive parts sampled.
9	Millers Falls	42.6011	72.37782	215	Erving Formation	Dark-gray, knobby-weathering, medium-grained amphibolite from a prominent ledge on the side of the slope, above Rt. 2. Sample is from the bottom edge of the outcrop.
BN-48 to BN-53	Bernardston?	-	-	-	Erving Formation	Amphibolite, collected and crushed by Bull (1997), but sample not analyzed and location not recorded.
A13-A	Ludlow	42.179	72.410	82	Belchertown Complex	Hornblende quartz monzodiorite, hydrated form of original rock. Sample location A13 of Ashwal (1974, fig. 5), also see Ashwal and others (1979).
A13-B	Ludlow	42.179	72.410	82	Belchertown Complex	Hornblende-pyroxene quartz monzodiorite, partially hydrated form of original rock. Sample location A13 of Ashwal (1974, fig. 5), also see Ashwal and others (1979).
A13-C	Ludlow	42.179	72.410	82	Belchertown Complex	Hornblende quartz monzodiorite, hydrated form of original rock. Sample location A13 of Ashwal (1974, fig. 5), also see Ashwal and others (1979).
A21-11	Ludlow	42.179	72.410	82	Belchertown Complex	Pyroxene quartz monzodiorite, with red plagioclase, original rock prior to metamorphic hydration. Sample location A21 of Ashwal (1974, fig. 5), also see Ashwal and others (1979).
A22-2Aa	Ludlow	42.179	72.410	82	Belchertown Complex	Pyroxene quartz monzodiorite, with red plagioclase, original rock prior to metamorphic hydration. Sample location A22 of Ashwal (1974, fig. 5), also see Ashwal and others (1979).
A22-2Ab	Ludlow	42.179	72.410	82	Belchertown Complex	Biotite tonalite, 3 cm thick dike cutting pyroxene quartz diorite. Sample location A22 of Ashwal (1974, fig. 5), also see Ashwal and others (1979).
Rt2H1	Templeton	42.5678	72.1123	324	Hardwick Pluton	Brooks Village Sill of Hardwick Pluton, garnet-biotite tonalite, long roadcut on south side of eastbound lane of Rt. 2.
Rt2H2	Athol	42.5763	72.16944	348	Hardwick Pluton	Main body of Hardwick biotite tonalite, road cut on north side of west-bound lane of Rt. 2.

[1]GPS latitude, longitude, and elevations use the WGS84 datum.

TABLE A3-1

New major element analyses of samples from the Cooleyville Gneiss, Packerd Gabbro, Fourmile Gneiss, Erving Formation, Belchertown Complex, and Hardwick Pluton

			Major elements, wt. %														LOI %
Body[1]	Rock[2]	Sample	SiO_2	TiO_2	Al_2O_3	Fe_2O_3	FeO	MnO	MgO	CaO	Na_2O	K_2O	P_2O_5	CO_2	S	Sum	
PP	PG	6B	48.15	0.36	18.73		8.36	0.12	9.63	12.19	2.16	0.12	0.02	0.11	0.75	100.72	2.0
PP	PG	4D3	48.16	1.81	16.91		9.57	0.17	8.85	11.52	2.39	0.17	0.12	<0.07	<0.02	99.67	0.6
PP	PG	10f	48.29	1.11	14.95		10.48	0.20	11.21	10.79	2.44	0.19	0.09	0.07	<0.02	99.83	0.9
PP	PG	6A	48.41	0.48	20.56		6.07	0.11	10.61	10.81	2.37	0.37	0.04	0.15	<0.02	99.98	2.7
PP	PG	2K5	48.65	3.52	15.55		13.61	0.26	5.56	9.11	2.80	0.28	0.42	0.07	<0.02	99.82	0.1
PP	PG	2I1b	48.76	3.70	17.74		13.39	0.25	4.47	7.38	2.69	0.69	0.74	0.11	0.02	99.92	1.0
PP	PG	BL	48.77	1.62	17.89		8.95	0.17	8.45	10.34	2.78	0.63	0.21	<0.07	<0.02	99.79	2.1
PP	PG	1I6	48.86	2.37	16.03		11.13	0.21	7.10	10.55	2.88	0.34	0.31	0.07	<0.02	99.85	0.8
PP	PG	8	48.94	0.92	21.19		6.21	0.12	7.20	11.87	2.55	0.67	0.09	0.07	0.02	99.85	1.5
PP	PG	2F4	49.43	1.38	17.91		8.21	0.15	8.07	10.92	3.19	0.33	0.15	<0.07	0.03	99.77	0.9
PP	PG	3	49.56	1.57	17.00		8.98	0.16	8.42	10.78	2.86	0.20	0.13	0.11	<0.02	99.78	0.8
PP	PG	3I7	49.70	1.84	17.32		9.75	0.17	7.95	10.82	1.87	0.13	0.20	0.11	0.13	100.00	1.0
PP	PG	1I3	49.70	1.72	17.14		9.27	0.17	7.87	9.86	3.13	0.70	0.18	0.11	0.03	99.89	1.0
PP	PG	46	49.71	2.35	16.71		11.33	0.26	7.45	10.34	1.13	0.20	0.30	0.26	0.04	100.08	1.6
PP	PG	2F6	49.88	1.39	18.14		7.82	0.14	7.83	11.11	2.92	0.36	0.14	0.15	<0.02	99.88	0.9
PP	PG	2I1a	49.98	2.50	16.90		11.30	0.27	6.32	9.43	2.44	0.27	0.31	<0.07	<0.02	99.70	0.7
PP	PG	C01	50.06	2.74	17.67		10.18	0.22	5.81	9.49	2.99	0.17	0.49	0.11	<0.02	99.94	0.5
PP	PG	2K3	50.18	1.89	17.20		9.52	0.17	6.81	10.69	2.82	0.28	0.20	<0.07	<0.02	99.76	0.5
PP	PG	2I1+100	50.29	1.53	17.06		8.79	0.16	7.77	10.10	3.09	0.74	0.16	0.07	<0.02	99.77	0.7
PP	PG	43A	50.58	0.99	17.75		7.60	0.14	8.51	10.87	2.72	0.47	0.10	0.07	0.03	99.84	1.6
PP	PG	10c	50.74	1.98	16.79		8.87	0.16	7.14	10.02	3.60	0.25	0.20	<0.07	<0.02	99.75	0.5
PP	PG	159	50.88	2.02	15.97		9.84	0.29	7.45	9.13	3.25	0.65	0.20	0.07	<0.02	99.76	1.2
PP	PG	2F8	53.43	3.08	14.94		14.26	0.25	4.22	7.39	1.33	0.54	0.29	<0.07	<0.02	99.74	-0.3
PP	PG	64	51.27	2.89	16.04		12.40	0.24	3.95	7.26	3.30	1.49	0.82	0.07	<0.02	99.75	0.2
PP	PG	11	51.28	1.67	17.00		8.52	0.17	7.41	9.83	2.79	0.81	0.21	<0.07	<0.02	99.70	1.1
PP	PG	4I7	51.63	0.71	17.64		6.56	0.14	8.42	12.56	1.93	0.18	0.07	<0.07	0.02	99.86	0.9
PP	PG	3I7A	51.73	1.75	17.39		9.21	0.24	7.46	9.23	2.00	0.56	0.21	0.15	<0.02	99.91	1.8
PP	PG	578	52.00	1.37	17.22		8.43	0.17	6.48	9.03	3.38	1.43	0.19	0.11	<0.02	99.82	0.6
PP	PG	233	53.17	1.53	17.45		8.20	0.16	6.81	9.22	2.44	0.59	0.19	0.07	0.03	99.87	1.6
PP	CG	B55Cb	63.14	0.77	16.17		6.05	0.12	1.82	4.26	3.83	3.30	0.31	<0.07	<0.02	99.78	0.5
PP	CG	B55B	63.35	0.81	16.30		5.61	0.11	1.74	4.40	3.73	3.37	0.37	<0.07	<0.02	99.80	0.6
PP	CG	B55A	63.97	0.89	16.10		5.44	0.09	1.52	3.97	3.75	3.71	0.32	<0.07	<0.02	99.76	0.8
PP	CG	65a	64.76	0.81	16.47		5.73	0.20	1.31	4.27	4.26	1.73	0.26	<0.07	<0.02	99.81	0.6
PP	CG	4F3	64.81	0.82	16.18		5.01	0.08	1.38	3.73	3.90	3.58	0.28	<0.07	<0.02	99.78	0.3
PP	CG	M82	65.26	0.83	16.47		3.87	0.12	1.85	3.46	5.91	1.73	0.31	0.40	<0.02	100.20	0.7
PP	CG	159A	65.62	0.85	16.78		4.57	0.07	2.21	3.24	2.89	3.33	0.23	0.11	0.07	99.97	2.2
PP	CG	5D2	66.12	0.82	15.87		5.53	0.10	1.24	2.33	3.66	3.81	0.29	0.07	<0.02	99.86	0.3
PP	CG	65b	66.21	0.64	16.30		4.31	0.12	1.21	3.67	3.58	3.49	0.23	0.11	0.05	99.92	0.6
PP	CG	69	66.96	0.64	16.24		4.33	0.07	1.24	2.88	4.32	2.96	0.21	<0.07	<0.02	99.86	0.7
PP	CG	74	68.68	0.47	15.62		3.43	0.04	0.84	2.54	3.77	4.32	0.14	0.11	<0.02	99.96	0.4
PP	CG	M83	68.74	0.73	15.16		4.25	0.12	1.38	2.56	5.00	1.63	0.20	0.11	0.04	99.94	1.4
PP	CG	6.5	69.02	0.62	16.27		3.94	0.07	1.41	2.27	3.26	2.83	0.15	0.11	<0.02	99.97	1.8
PP	CG	40	69.38	0.52	15.83		2.80	0.08	0.98	2.48	5.14	2.50	0.13	<0.07	<0.02	99.84	0.4
PP	CG	B57	69.44	15.08	0.45		3.40	0.05	0.72	2.35	3.67	4.43	0.13			99.72	

TABLE A3-1
(continued)

Body[1]	Rock[2]	Sample	Major elements, wt. % SiO_2	TiO_2	Al_2O_3	Fe_2O_3	FeO	MnO	MgO	CaO	Na_2O	K_2O	P_2O_5	CO_2	S	Sum	LOI %
PP	CG	B57b	69.68	0.43	15.07		3.19	0.05	0.71	2.24	3.66	4.62	0.13	<0.07	<0.02	99.80	0.6
PP	CG	39	70.28	0.55	15.00		2.91	0.07	0.68	1.36	4.20	4.73	0.10	0.11	<0.02	99.99	0.7
PP	CG	75	70.51	0.43	14.91		3.16	0.03	0.71	2.15	3.62	4.21	0.13	0.11	<0.02	99.96	0.4
PP	CG	362	70.89	0.50	15.76		2.33	0.06	0.83	3.82	4.71	0.87	0.11	0.11	<0.02	99.98	0.5
PP	CG	0I6	70.99	0.14	15.85		3.41	0.13	0.10	1.55	5.86	1.76	0.05	0.11	<0.02	99.96	0.5
PP	CG	18	71.08	0.44	14.57		3.16	0.05	0.48	1.68	3.64	4.54	0.07	0.11	<0.02	99.84	0.5
PP	CG	747	71.34	0.31	14.82		3.79	0.15	0.84	3.45	4.42	0.72	0.08	0.07	<0.02	99.99	0.3
PP	CG	KH	71.41	0.30	14.64		2.73	0.04	0.44	1.48	3.73	4.93	0.07	<0.07	<0.02	99.78	0.3
PP	CG	5IOA	71.52	0.37	14.46		2.91	0.03	0.61	1.97	3.66	4.13	0.11	0.07	<0.02	99.85	0.4
PP	CG	729	71.84	0.34	14.69		3.56	0.11	0.91	2.19	4.79	1.41	0.11	<0.07	<0.02	99.94	0.4
PP	CG	6D6	72.18	0.30	14.27		2.45	0.04	0.48	1.49	3.53	4.93	0.08	<0.07	<0.02	99.75	0.4
PP	CG	B08	72.71	0.21	14.22		3.97	0.14	0.58	3.24	3.13	1.61	0.05	<0.07	<0.02	99.86	0.5
PP	CG	5E3	75.66	0.13	13.37		2.02	0.06	0.22	1.10	4.30	2.92	0.04	<0.07	<0.02	99.81	0.3
PP	CG	B56	75.74	0.18	13.99		1.50	0.06	0.25	0.68	6.31	1.05	0.09	0.11	<0.02	99.97	0.2
PP	CG	4I9A	75.76	0.14	12.95		1.31	0.01	0.16	0.89	3.19	5.35	0.03	0.07	<0.02	99.87	0.4
PP	CG	B10	76.16	0.16	12.98		2.03	0.07	0.66	0.98	3.96	2.88	0.03	0.18	<0.02	100.09	0.9
TAPC	FMG	1	81.13	0.06	11.69	0.05	0.75	0.01	0.44	0.68	4.03	1.50	0.03			100.37	
TAPC	FMG	4	77.89	0.07	12.33	0.23	0.79	0.08	0.21	1.32	3.62	2.79	0.01			99.34	
TAPC	FMG	5	78.19	0.08	12.68	0.25	0.79	0.07	0.30	1.35	4.41	1.58	0.02			99.72	
TAPC	FMG	7	74.83	0.19	14.16	0.20	2.01	0.03	1.33	1.07	4.54	1.89	0.04			100.29	
TAPC	FMG	8	78.16	0.12	13.20	0.33	0.99	0.01	0.54	1.17	4.59	1.25	0.03			100.40	
TAPC	FMG	10	79.20	0.05	12.72	0.05	0.75	0.01	0.50	0.96	3.86	1.82	0.19			100.12	
TAPC	FMG	17	79.07	0.07	11.84	0.16	0.80	0.03	0.45	0.87	3.57	2.46	0.02			99.34	
TAPC	FMG	19	78.47	0.07	11.92	0.12	0.97	0.05	0.31	0.40	1.75	5.95	0.02			100.02	
TAPC	FMG	20	79.05	0.07	12.04	0.20	0.59	0.05	0.24	0.61	2.05	5.47	0.01			100.39	
TAPC	FMG	22	76.13	0.10	13.73	0.15	1.13	0.08	0.42	2.27	4.42	1.59	0.02			100.04	
TAPC	FMG	23															
TAPC	FMG	25	78.45	0.20	11.66	1.00	1.38	0.04	0.61	2.36	3.59	0.57	0.02			99.89	
TAPC	FMG	26	76.89	0.12	13.05	0.71	0.99	0.06	0.48	1.87	3.84	2.46	0.03			100.49	
TAPC	FMG	29	77.89	0.07	12.81	0.19	1.00	0.06	0.26	1.90	4.11	1.82	0.03			100.14	
TAPC	FMG	33	77.15	0.10	12.97	0.31	0.79	0.04	0.55	1.71	4.49	1.18	0.01			99.31	
TAPC	FMG	34	77.83	0.10	12.80	0.33	0.70	0.03	0.55	1.72	4.63	1.09	0.01			99.80	
TAPC	FMG	36	76.31	0.19	13.67	0.16	1.74	0.10	0.83	1.72	4.87	0.83	0.04			100.46	
TAPC	FMG	37	78.10	0.04	12.75	0.33	0.89	0.06	0.62	2.81	2.47	2.29	0.01			100.38	
TAPC	FMG	38	74.61	0.16	14.10	0.67	1.50	0.08	0.61	2.59	3.93	2.15	0.04			100.42	
TAPC	FMG	41	78.09	0.06	12.51	0.52	0.55	0.09	0.23	1.08	4.44	2.11	0.01			99.70	
TAPC	FMG	42	77.58	0.06	12.73	0.38	0.68	0.06	0.17	1.05	4.24	2.97	0.01			99.93	
TAPC	FMG	48	63.37	0.50	15.73	0.40	5.99	0.18	2.83	5.23	2.83	2.59	0.08			99.73	
TAPC	FMG	50															
TAPC	FMG	51															
TAPC	FMG	52															
TAPC	FMG	53															
TAPC	FMG	54															
TAPC	FMG	55															
TAPC	FMG	57	50.99	0.71	18.10	1.01	8.20	0.18	6.46	9.75	3.67	0.48	0.13			99.67	
TAPC	FMG	58	51.07	0.95	17.00	1.56	7.39	0.20	7.38	10.54	3.36	0.32	0.13			99.91	

TABLE A3-1
(continued)

			Major elements, wt. %														LOI %
Body[1]	Rock[2]	Sample	SiO_2	TiO_2	Al_2O_3	Fe_2O_3	FeO	MnO	MgO	CaO	Na_2O	K_2O	P_2O_5	CO_2	S	Sum	
TAPC	FMG	61	55.66	0.69	15.50	2.97	7.97	0.23	5.16	7.13	4.51	0.22	0.06			100.12	
TAPC	FMG	62	52.01	0.42	15.19	2.92	7.38	0.23	8.70	8.90	3.57	0.44	0.07			99.83	
TAPC	FMG	JB-06	49.31	0.45	15.64	13.39		0.22	6.20	11.23	1.59	0.54	0.02	0.22	<0.02	98.81	1.2
TAPC	FMG	JB-13	75.94	0.06	13.05	0.93		0.03	0.33	0.56	3.11	5.50	0.02	0.22	<0.02	99.75	0.3
Erving3	Amph	2	48.23	1.24	15.88	10.44		0.17	8.74	12.70	2.12	0.20	0.08		0.01	99.81	0.7
Erving3	Amph	5	48.06	1.13	16.58	9.73		0.18	8.08	12.97	2.68	0.31	0.09		0.01	99.82	0.9
Erving3	Amph	7	48.85	1.33	15.19	11.23		0.20	8.36	11.55	2.66	0.35	0.08		0.01	99.81	0.7
Erving3	Amph	9	50.11	0.58	15.79	7.54		0.13	10.05	13.77	1.68	0.13	0.02		0.01	99.81	1.1
Erving	Amph	BN-48	48.06	2.29	14.10	13.78		0.24	6.49	11.14	2.63	0.36	0.22	<0.07	<0.02	99.31	0.5
Erving	Amph	BN-49	49.25	1.84	13.60	12.45		0.19	6.98	10.70	3.07	0.44	0.18	0.73	0.03	99.46	1.1
Erving	Amph	BN-50	48.24	3.33	12.00	17.98		0.25	5.44	9.46	2.32	0.22	0.33	0.07	<0.02	99.64	0.2
Erving	Amph	BN-51	48.84	2.09	13.94	14.23		0.18	6.95	9.08	2.53	1.04	0.18	<0.07	<0.02	99.06	0.6
Erving	Amph	BN-52	47.52	1.17	16.58	10.10		0.17	7.12	13.22	2.63	0.24	0.08	<0.07	<0.02	98.83	0.9
Erving	Amph	BN-53	46.92	0.93	15.87	9.06		0.16	8.75	13.59	2.43	0.39	0.06	0.81	<0.02	98.97	1.6
BC	QzMzd	A13-A	59.02	0.53	15.86	4.55		0.07	4.80	5.69	3.64	3.74	0.47			98.37	0.90
BC	QzMzd	A13-B	58.36	0.71	15.38	5.23		0.08	5.37	6.23	3.59	2.98	0.49			98.42	0.90
BC	QzMzd	A13-C	58.32	0.72	15.43	5.21		0.08	5.38	6.05	3.57	3.21	0.48			98.45	0.90
BC	QzMzd	A21-11	57.81	0.64	15.21	5.50		0.09	5.80	6.89	3.79	2.80	0.56			99.09	0.20
BC	QzMzd	A22-2Aa	57.27	0.67	15.14	5.64		0.09	5.98	6.87	3.61	2.87	0.57			98.71	0.60
BC	T	A22-2Ab	68.95	0.29	16.67	1.56		0.02	1.22	4.19	5.36	1.06	0.10			99.42	0.30
HP	TG	Rt2H1	63.29	1.03	16.50	6.15		0.09	2.46	3.17	3.46	2.62	0.22			98.99	0.8
HP	T	Rt2H2	55.41	2.57	15.00	9.05		0.23	3.96	5.16	2.92	3.46	0.98			98.74	0.7

[1]Body abbreviations: PP, Prescott Peninsula; TAPC, Taconian arc plutonic complex; Erving, Erving Formation amphibolites; BC, Belchertown Complex; HP, Hardwick Pluton.

[2]Rock abbreviations: PG, Packard Gabbro; CG, Cooleyville Gneiss; FMG, Fourmile Gneiss; Amph, amphibolite; QzMzd, quartz monzodiorite; TG, garnet-bearing tonalite; T, tonalite.

[3]Sulfur by ICP-MS, oxygen mass-shift mode.

TABLE A3-2

New trace element analyses of samples from the Cooleyville Gneiss, Packerd Gabbro, Fourmile Gneiss, Erving Formation, Belchertown Complex, and Hardwick Pluton

			Trace elements, ppm																																						
Body[1]	Rock[2]	Sample	Li	Be	Sc	V	Cr	Co	Ni	Cu	Zn	Ga	Rb	Sr	Y	Zr	Nb	Mo	Sn	Sb	Cs	Ba	La	Ce	Pr	Nd	Sm	Eu	Gd	Tb	Dy	Ho	Er	Tm	Yb	Lu	Hf	Ta	Pb	Th	U
PP	PG	6B	11.5	0.2	19.1	66.2	306.9	51.8	192.4	138.7	50.5	12.6	1.8	276	5.0	11	0.3	0.14	0.97	0.12	0.24	11	1.3	3.4	0.51	2.5	0.73	0.63	0.89	0.15	0.92	0.19	0.51	0.07	0.47	0.08	0.34	0.03	3.1	0.07	0.03
PP	PG	4D3	11.3	0.4	38.9	183.1	320.2	38.0	54.9	24.3	76.3	16.3	2.0	290	24.2	68	2.4	0.05	0.24	0.08	0.05	46	4.5	12.8	2.14	11.2	3.38	1.46	4.10	0.68	4.24	0.86	2.30	0.33	2.07	0.32	1.86	0.16	3.4	0.21	0.06
PP	PG	10f	15.6	0.5	36.2	160.8	122.1	51.0	69.2	4.8	94.8	14.4	2.3	241	20.4	73	2.1	0.08	0.95	0.13	0.10	25	4.6	13.2	2.05	10.3	2.90	1.13	3.44	0.56	3.54	0.73	1.97	0.29	1.86	0.30	1.83	0.13	3.8	0.62	0.19
PP	PG	6A	11.8	0.3	13.5	69.2	194.3	39.9	150.9	13.7	44.0	11.6	16.1	295	6.9	27	1.1	0.05	0.46	0.08	1.43	41	2.2	5.5	0.81	3.8	1.05	0.61	1.21	0.20	1.21	0.26	0.71	0.10	0.65	0.10	0.71	0.07	3.4	0.23	0.10
PP	PG	2K5	18.5	1.0	39.5	276.2	28.7	28.4	9.6	12.1	148.3	21.9	2.3	275	53.6	304	13.8	0.29	0.98	0.15	0.08	124	17.8	44.4	6.44	30.4	8.22	2.65	9.35	1.50	9.33	1.91	5.24	0.77	4.95	0.80	6.07	0.81	4.8	0.62	0.29
PP	PG	2I1b	20.6	0.7	40.2	335.1	51.7	20.5	12.4	23.5	167.3	26.3	18.3	239	66.9	189	25.4	0.79	0.35	0.07	1.40	317	31.5	75.9	10.84	49.3	12.61	3.24	12.37	1.99	11.81	2.36	6.25	0.88	5.39	0.83	4.23	1.55	6.8	1.08	0.55
PP	PG	BL	32.2	0.9	26.7	226.3	258.2	38.3	90.9	28.4	68.4	16.0	34.0	304	25.4	132	4.4	0.19	1.41	0.10	0.61	26	7.9	20.5	3.00	14.5	3.97	1.43	4.57	0.74	4.53	0.94	2.63	0.38	2.42	0.38	3.14	0.31	5.2	0.58	0.20
PP	PG	1I6	14.1	0.8	40.9	310.7	189.8	30.4	26.5	15.2	97.9	18.7	5.0	276	41.2	158	6.8	0.17	1.26	0.14	0.44	78	12.6	32.9	4.76	23.1	6.09	1.93	7.09	1.14	7.18	1.50	4.07	0.59	3.85	0.60	3.94	0.42	3.5	0.72	0.23
PP	PG	8	16.0	0.6	23.5	113.3	178.0	33.9	76.5	16.0	57.5	15.4	27.5	326	18.3	105	2.5	0.10	1.08	0.09	1.69	140	6.3	15.7	2.19	10.3	2.65	0.99	3.03	0.50	3.15	0.65	1.81	0.27	1.76	0.27	2.37	0.17	5.0	1.50	0.43
PP	PG	2F4	11.1	0.6	32.8	186.2	275.1	40.8	67.8	40.0	62.4	16.5	6.6	294	25.5	122	3.0	0.15	1.07	0.15	0.36	40	6.7	18.0	2.69	13.0	3.70	1.34	4.34	0.72	4.50	0.94	2.55	0.38	2.38	0.38	2.98	0.21	1.6	0.75	0.20
PP	PG	3	5.7	0.5	35.1	225.8	241.9	38.7	79.5	14.1	81.7	16.0	3.1	257	27.4	81	2.3	0.12	0.72	0.08	0.10	63	6.2	16.8	2.69	13.3	3.89	1.42	4.55	0.77	4.78	1.01	2.70	0.39	2.55	0.39	2.22	0.16	3.7	0.56	0.15
PP	PG	3I7	26.5	0.8	30.1	272.1	287.7	36.3	65.0	31.9	73.7	17.3	1.6	270	29.9	133	5.3	0.53	0.58	0.16	0.21	24	10.6	25.4	3.62	17.0	4.74	1.63	5.34	0.89	5.47	1.13	3.10	0.45	2.96	0.46	3.34	0.35	4.7	0.67	0.22
PP	PG	1I3	19.6	0.9	33.9	227.6	253.7	40.2	71.0	33.7	82.4	18.3	23.2	279	31.6	144	4.9	0.40	1.53	0.12	1.47	108	9.8	24.8	3.59	16.9	4.58	1.55	5.30	0.85	5.29	1.11	3.04	0.46	2.93	0.46	3.51	0.31	4.8	1.52	0.41
PP	PG	46	16.1	0.9	38.9	343.5	205.7	39.9	46.2	9.4	105.3	19.5	3.4	158	37.5	169	7.0	0.12	1.52	0.16	0.15	28	12.2	30.2	4.35	20.4	5.55	2.00	6.44	1.06	6.59	1.38	3.74	0.55	3.56	0.57	3.74	0.43	4.0	0.38	0.14
PP	PG	2F6	12.7	0.7	27.6	191.3	278.3	28.6	51.2	27.7	58.7	15.6	9.9	275	25.8	128	2.2	0.24	1.52	0.09	0.73	54	7.1	18.8	2.85	13.6	3.97	1.41	4.58	0.76	4.72	0.99	2.70	0.39	2.56	0.40	3.23	0.16	2.8	1.16	0.29
PP	PG	2I1a	16.8	1.2	38.6	332.9	166.0	29.7	28.8	7.3	105.7	20.8	4.3	254	40.1	186	11.0	0.46	0.21	0.10	0.19	72	14.6	34.8	5.03	23.6	6.56	2.32	7.14	1.19	7.40	1.53	4.20	0.61	3.96	0.63	4.20	0.71	5.6	0.45	0.23
PP	PG	C01	9.5	0.8	29.0	326.5	28.7	23.2	9.5	5.9	87.0	17.2	1.2	304	23.8	69	12.2	0.23	0.19	0.09	0.03	73	12.2	27.5	3.88	18.5	4.81	2.21	5.25	0.78	4.62	0.94	2.53	0.35	2.27	0.37	1.57	0.77	4.4	0.24	0.10
PP	PG	2K3	11.1	0.6	34.8	265.9	173.7	28.5	24.9	15.3	84.0	18.4	3.3	264	33.2	89	4.8	0.07	1.16	0.13	0.13	100	11.3	28.1	4.09	19.3	5.17	1.62	5.84	0.93	5.87	1.21	3.28	0.48	3.10	0.50	2.46	0.30	3.4	0.61	0.20
PP	PG	2I1+100	17.4	0.8	35.9	172.8	310.9	34.3	55.2	17.8	75.3	17.4	33.5	271	28.1	134	5.2	0.23	1.43	0.09	2.20	124	10.8	25.3	3.45	15.4	4.14	1.36	4.82	0.80	4.88	1.02	2.75	0.41	2.62	0.41	3.33	0.34	5.4	2.07	0.59
PP	PG	43A	19.6	0.6	30.0	166.0	451.6	35.9	66.6	38.1	52.3	14.6	18.7	314	19.2	80	3.3	0.07	1.09	0.09	1.22	108	8.1	19.0	2.60	11.6	3.08	1.07	3.39	0.56	3.41	0.70	1.92	0.28	1.78	0.28	2.07	0.23	4.4	1.36	0.32
PP	PG	10c	8.4	1.0	45.3	239.8	63.4	33.8	31.6	15.7	83.8	18.9	6.3	401	30.5	175	4.4	0.07	1.08	0.11	0.23	50	9.7	25.7	3.49	16.3	4.59	1.48	5.36	0.87	5.34	1.09	2.94	0.42	2.71	0.42	4.02	0.26	7.2	2.16	0.49
PP	PG	159	14.3	0.6	41.7	266.5	215.0	21.0	26.9	3.3	114.4	15.7	21.3	266	30.2	52	5.3	0.05	1.43	0.18	0.33	280	13.8	31.9	4.75	23.2	6.05	1.92	6.15	0.94	5.67	1.17	3.19	0.45	2.95	0.47	1.71	0.29	4.1	0.69	0.18
PP	PG	2F8	21.9	1.4	44.0	411.7	36.0	38.6	13.4	9.6	116.8	25.2	24.0	208	59.4	286	10.9	0.57	3.16	0.13	1.28	211	21.8	49.9	6.94	31.3	8.36	2.85	9.68	1.59	9.85	2.09	5.80	0.88	5.72	0.91	7.19	0.70	5.0	4.17	1.18
PP	PG	64	20.0	2.2	32.7	316.0	32.1	18.4	5.8	12.4	164.0	25.3	49.8	206	100.0	638	23.1	1.00	3.74	0.05	1.39	481	59.1	134.3	18.59	81.2	19.77	4.10	20.25	3.11	18.36	3.79	10.45	1.52	9.90	1.57	15.46	1.30	13.0	4.42	1.71
PP	PG	11	15.5	1.0	32.6	212.1	238.2	35.1	65.0	26.0	79.5	17.5	23.2	294	32.1	168	6.3	0.41	1.57	0.10	0.54	178	12.7	30.1	4.32	19.6	5.02	1.60	5.69	0.94	5.81	1.21	3.26	0.48	3.11	0.48	3.99	0.43	5.2	1.91	0.60
PP	PG	4I7	11.8	0.4	37.0	160.2	176.5	32.9	61.8	21.0	58.3	15.4	5.9	251	15.8	37	1.7	0.09	0.45	0.05	0.52	33	4.6	10.8	1.56	7.4	2.07	0.85	2.50	0.43	2.68	0.56	1.53	0.23	1.50	0.24	1.03	0.11	3.9	0.57	0.19
PP	PG	3I7A	26.3	1.1	31.6	211.6	223.6	35.2	67.0	5.7	104.9	18.2	21.3	268	31.4	146	7.2	0.29	1.00	0.16	1.12	131	13.7	31.7	4.39	20.0	5.04	1.77	5.55	0.91	5.65	1.16	3.17	0.46	2.95	0.46	3.48	0.47	5.7	2.67	0.76
PP	PG	578	16.8	1.2	23.4	210.9	190.3	27.7	29.8	10.2	89.2	17.0	44.4	194	35.6	144	5.5	0.26	3.26	0.04	1.84	212	18.3	41.3	5.42	23.1	5.76	1.73	6.22	1.01	6.25	1.33	3.75	0.55	3.61	0.59	3.88	0.37	11.5	2.69	0.85
PP	PG	233	27.7	0.9	33.5	201.0	217.0	41.0	63.8	27.6	88.9	19.7	34.6	352	32.9	204	5.5	0.12	1.10	0.29	1.34	145	21.2	44.5	5.73	24.4	5.66	1.94	6.06	0.94	5.78	1.18	3.25	0.47	3.15	0.50	4.95	0.38	8.2	2.70	0.77
PP	CG	B55Cb	25.5	2.1	16.7	73.4	1.1	8.3	2.6	0.8	37.9	18.8	169.1	170	38.9	187	12.2	0.14	2.70	0.05	2.26	505	50.3	117.6	14.06	56.0	11.12	1.76	9.26	1.23	7.08	1.44	4.01	0.62	4.19	0.68	5.26	0.59	5.1	18.82	3.29
PP	CG	B55B	23.3	2.0	15.2	48.0	0.4	8.5	1.9	1.1	41.9	18.5	167.6	190	34.1	184	11.9	0.50	2.46	0.04	2.46	607	47.5	107.0	13.04	50.5	9.51	1.89	7.62	1.04	5.81	1.18	3.24	0.49	3.34	0.54	4.84	0.57	4.6	18.38	3.78
PP	CG	B55A	15.4	1.8	17.5	43.6	0.5	7.2	1.5	1.1	37.3	19.2	165.1	195	37.3	171	14.9	0.46	1.97	0.04	1.62	718	53.2	110.1	13.45	52.8	9.85	2.00	8.00	1.09	6.27	1.29	3.63	0.55	3.69	0.59	4.66	0.76	6.6	19.50	3.48
PP	CG	65a	18.9	1.9	16.4	29.0	0.5	4.5	1.7	2.4	60.1	19.4	68.2	277	31.6	163	13.4	0.20	2.11	0.04	1.47	764	44.9	94.0	11.66	44.2	8.22	2.01	6.66	0.98	5.75	1.19	3.30	0.51	3.34	0.55	4.71	0.78	7.2	17.05	3.06
PP	CG	4F3	11.7	1.9	15.2	61.9	0.4	5.2	1.3	2.6	24.7	19.5	147.3	212	31.7	195	15.5	0.48	3.46	0.04	2.44	801	58.2	115.9	13.75	51.7	8.61	1.88	7.06	0.93	5.40	1.10	3.02	0.47	3.09	0.51	5.15	0.92	3.7	19.74	3.85
PP	CG	M82	15.0	1.5	13.3	78.1	2.3	5.6	2.7	0.0	21.2	17.2	59.7	167	35.0	197	11.5	0.07	6.70	0.07	1.40	359	38.6	88.7	11.72	47.6	9.49	2.23	7.76	1.06	6.11	1.25	3.52	0.53	3.54	0.58	5.32	0.62	4.5	17.67	2.76
PP	CG	159A	17.7	1.8	10.2	61.4	44.9	13.3	26.0	22.0	85.6	22.6	120.3	219	25.1	302	14.8	0.56	1.45	0.04	1.12	677	47.3	97.9	12.29	48.6	9.67	1.85	7.68	0.95	4.79	0.88	2.26	0.32	2.05	0.31	7.71	0.93	14.9	14.37	2.58
PP	CG	5D2	39.5	3.0	14.9	68.6	20.7	6.6	7.2	7.8	80.3	22.8	161.4	101	41.4	405	15.1	1.02	4.68	0.03	5.44	607	19.1	45.6	6.15	26.3	5.35	1.02	4.80	0.84	6.04	1.47	4.64	0.78	5.56	0.92	10.58	1.01	20.3	17.55	3.31
PP	CG	65b	8.7	1.8	12.1	45.7	0.9	6.1	1.8	3.7	54.8	17.5	115.3	194	28.0	197	13.0	0.17	2.25	0.05	1.09	946	35.2	73.6	8.76	32.5	6.03	1.40	4.98	0.74	4.67	0.99	2.88	0.47	3.23	0.53	5.37	0.72	6.7	20.98	3.48
PP	CG	69	9.8	2.1	10.4	40.6	1.0	3.1	1.4	1.5	24.8	17.2	161.4	164	22.4	203	14.2	0.24	4.64	0.03	2.86	562	18.1	52.1	3.11	11.1	2.34	0.79	2.42	0.41	3.07	0.77	2.51	0.42	2.97	0.49	5.53	0.70	4.3	18.83	2.18

TABLE A3-2
(continued)

			Trace elements, ppm																																					
Body[1]	Rock[2]	Sample	Li	Be	Sc	V	Cr	Co	Ni	Cu	Zn	Ga	Rb	Sr	Y	Zr	Nb	Mo	Sn	Sb	Cs	Ba	La	Ce	Pr	Nd	Sm	Eu	Gd	Tb	Dy	Ho	Er	Tm	Yb	Lu	Hf	Ta	Pb	Th	U
PP	CG	74	19.5	1.9	9.0	33.2	1.4	3.4	1.7	1.6	15.2	16.3	169.9	147	27.7	229	13.7	0.42	2.86	0.02	2.35	889	18.2	37.0	4.46	17.8	4.32	0.99	4.24	0.70	4.54	0.98	2.89	0.45	3.15	0.53	6.16	0.81	3.6	21.15	3.50
PP	CG	M83	14.6	1.8	12.7	37.9	1.8	3.9	2.1	3.3	22.1	17.5	42.2	112	33.9	228	13.2	0.03	2.95	0.07	0.59	972	51.2	100.4	12.54	48.4	8.97	1.98	7.30	0.97	5.48	1.14	3.30	0.51	3.54	0.61	6.17	0.74	3.2	18.91	3.33
PP	CG	6.5	37.4	2.2	9.2	61.7	23.6	9.3	13.3	17.0	81.4	21.9	86.8	156	43.3	250	12.8	0.52	2.88	0.04	1.23	551	57.6	89.7	13.52	53.4	10.47	1.71	9.71	1.36	7.53	1.47	3.91	0.57	3.64	0.58	7.11	0.80	22.2	15.24	2.99
PP	CG	40	3.1	2.0	9.4	32.5	1.8	4.7	1.9	3.5	26.2	16.6	90.0	118	34.2	257	14.6	0.14	5.75	0.02	0.71	755	50.5	98.5	12.18	45.5	7.72	1.29	6.12	0.90	5.71	1.24	3.65	0.58	3.98	0.65	7.07	0.85	4.5	26.02	4.29
PP	CG	B57				27.0	1.0		6.0		24.0			135		203	13.7					840	40.0	78.0																	
PP	CG	B55Ca	10.3	1.6	8.0	16.4	0.6	3.4	1.4	0.7	14.5	14.9	165.9	166	25.8	242	10.0	0.22	2.24	0.06	1.15	1364	31.2	63.5	7.63	29.5	5.70	1.56	4.72	0.69	4.14	0.88	2.59	0.41	2.90	0.47	6.35	0.64	7.9	24.93	3.26
PP	CG	B57b	11.4	2.0	8.6	20.5	1.1	3.9	2.1	0.3	18.8	16.7	179.2	127	32.8	234	14.6	0.75	3.31	0.01	3.04	807	50.9	92.7	11.98	43.4	7.72	1.34	6.11	0.92	5.55	1.17	3.38	0.54	3.62	0.60	6.41	0.93	4.1	22.94	4.28
PP	CG	39	29.9	1.9	7.3	17.5	0.5	2.2	1.0	2.5	16.9	14.2	120.3	119	35.4	259	14.1	0.14	1.22	0.03	2.13	1150	39.1	83.2	9.68	36.7	7.55	1.30	6.63	0.99	6.05	1.30	3.80	0.60	4.10	0.67	7.29	0.84	6.0	23.29	3.76
PP	CG	75	11.2	2.0	8.6	23.5	0.9	4.0	1.4	4.4	16.3	16.4	161.0	131	25.6	238	14.2	2.26	4.19	0.02	2.32	810	35.0	72.2	8.76	31.4	5.54	1.01	4.50	0.68	4.32	0.93	2.86	0.47	3.17	0.53	6.69	0.91	4.2	24.10	4.00
PP	CG	362	12.6	2.0	8.5	23.6	1.4	3.1	2.2	0.4	6.3	16.0	32.8	177	34.9	269	14.7	0.09	2.30	0.08	0.36	109	56.7	104.6	13.57	50.6	8.88	1.56	7.21	1.00	6.04	1.27	3.64	0.57	3.94	0.65	7.51	0.86	1.9	24.14	3.92
PP	CG	0I6	25.1	3.9	1.4	0.5	0.5	0.8	0.8	1.5	105.4	26.8	43.0	109	69.0	351	16.9	1.68	2.58	0.00	5.43	668	64.1	124.4	16.78	62.4	12.27	2.21	10.95	1.72	10.71	2.38	7.54	1.33	9.66	1.60	10.86	1.24	10.7	16.33	3.06
PP	CG	18	9.6	1.6	8.6	8.2	2.5	3.5	2.3	0.3	20.6	15.4	107.6	134	34.0	276	14.7	0.17	1.70	0.06	0.80	1752	39.5	92.3	9.26	34.3	6.50	1.30	5.67	0.85	5.46	1.19	3.54	0.57	3.99	0.66	7.44	0.84	25.9	20.30	3.54
PP	CG	747	10.2	0.9	15.1	13.0	0.7	4.4	1.1	0.3	69.5	15.0	23.3	147	26.2	102	2.8	0.04	0.73	0.11	0.66	209	16.6	29.0	3.88	15.4	3.40	0.93	3.69	0.61	3.97	0.90	2.64	0.42	2.89	0.48	2.89	0.15	8.5	3.39	0.79
PP	CG	KH	9.3	2.0	6.7	16.9	0.7	3.0	1.5	2.4	19.8	15.9	173.6	113	27.5	255	14.1	0.11	3.10	0.02	1.64	979	44.2	91.8	9.89	35.6	5.77	1.02	4.53	0.66	4.17	0.92	2.77	0.47	3.26	0.55	6.78	0.89	5.9	27.08	3.67
PP	CG	5IOA	22.5	1.9	7.6	23.5	1.7	2.8	1.7	7.1	17.5	15.9	174.0	134	27.9	247	11.3	0.54	3.76	0.02	2.81	861	31.5	73.8	6.98	25.7	4.84	1.04	4.33	0.69	4.44	0.96	2.84	0.46	3.21	0.53	6.67	0.79	5.6	29.19	3.83
PP	CG	729	18.0	0.9	11.9	10.5	0.4	3.6	0.9	0.3	54.7	13.7	50.0	85	19.2	91	2.4	0.02	0.64	0.01	2.47	234	11.7	26.3	2.96	12.0	2.70	0.86	2.85	0.47	3.12	0.67	2.00	0.32	2.16	0.36	2.58	0.14	10.1	2.83	0.80
PP	CG	6D6	16.6	2.0	5.5	16.7	1.0	3.1	1.6	0.8	16.4	15.9	213.3	99	33.7	199	13.1	0.08	2.59	0.04	3.41	896	86.1	119.4	18.23	63.4	10.07	1.36	7.59	1.02	5.86	1.17	3.30	0.51	3.48	0.58	5.36	0.78	4.2	26.68	4.07
PP	CG	B08	11.7	1.2	15.5	0.8	0.3	1.7	0.8	0.4	74.3	17.1	52.2	98	28.0	88	3.0	0.02	1.17	0.06	1.24	318	15.6	30.4	3.96	17.0	4.27	1.07	4.86	0.77	4.78	1.03	2.92	0.45	3.10	0.52	2.75	0.18	3.3	3.40	0.65
PP	CG	5E3	19.6	1.2	3.1	1.4	0.4	1.8	1.1	2.2	25.1	13.3	96.9	90	22.3	107	5.1	0.63	1.26	0.01	1.42	821	25.1	47.3	5.03	18.1	3.39	0.54	3.15	0.48	3.21	0.73	2.26	0.40	3.01	0.52	3.49	0.41	9.1	17.20	2.12
PP	CG	B56	11.6	1.2	3.9	2.1	0.3	1.1	0.9	0.3	53.5	10.9	27.6	116	20.6	110	3.1	0.12	1.12	0.02	2.12	405	13.8	26.2	3.50	13.8	3.00	0.81	3.00	0.49	3.23	0.73	2.25	0.37	2.55	0.43	3.29	0.19	9.8	3.93	1.25
PP	CG	4I9A	3.7	1.8	3.2	3.8	1.0	1.9	1.0	13.3	6.1	13.5	148.8	86	23.5	164	11.8	0.89	4.04	0.02	0.79	765	38.1	74.3	8.31	28.4	4.72	0.54	3.86	0.59	3.71	0.82	2.53	0.41	2.84	0.48	5.11	0.86	4.7	31.23	4.20
PP	CG	B10	13.0	1.0	10.7	9.2	1.3	2.4	1.1	0.2	51.0	12.1	57.7	162	23.1	113	3.7	0.01	1.63	0.02	2.61	545	21.0	39.3	4.82	18.8	4.18	0.92	4.18	0.64	3.95	0.82	2.31	0.36	2.41	0.41	3.36	0.25	9.6	5.62	1.36
TAPC	FMG	1	20.6	1.6	2.7	1.4	0.5		0.5	1.0	26.1	8.8	49.9	140	13.5	70	3.5		4.22	0.01	1.14	300	27.6	51.3	5.49	19.5	3.17	0.43	2.89		2.17		1.39		1.46	0.25	2.66		62.6	9.63	2.10
TAPC	FMG	4	8.3	1.3	5.3	2.2	0.2		1.4	3.3	26.9	10.9	75.6	64	31.5	95	3.2		1.00	0.01	0.71	662	8.0	14.2	1.80	6.8	1.64	0.38	2.15		4.05		3.81		4.79	0.83	3.82		24.7	6.23	1.51
TAPC	FMG	5	25.4	1.4	5.3	1.8	0.3		2.6	1.9	25.5	11.9	42.1	75	28.0	80	4.6		2.82	0.01	1.19	270	28.1	54.1	6.11	22.7	4.09	0.49	3.81		3.36		2.69		3.72	0.68	2.91		39.4	8.93	1.65
TAPC	FMG	7	32.7	1.3	10.1	25.4	0.6		1.6	3.6	60.0	13.6	89.6	143	15.7	89	4.5		5.19	0.01	3.67	353	16.8	33.7	3.56	12.5	2.21	0.62	2.26		2.14		1.47		1.57	0.25	2.49		57.2	6.02	1.85
TAPC	FMG	8	16.9	1.4	3.7	3.7	0.2		2.5	8.0	43.7	11.9	51.8	222	8.3	114	5.4		2.98	0.00	1.36	371	48.8	86.5	8.93	30.0	4.23	1.22	3.86		2.05		0.99		0.95	0.13	3.19		45.4	11.56	1.80
TAPC	FMG	10	28.6	1.5	10.5	1.5	0.6		0.6	0.9	28.4	12.2	62.6	147	14.7	77	5.1		4.42	0.08	1.48	396	28.7	54.8	6.05	22.4	4.22	0.77	3.73		3.02		1.46		1.37	0.22	3.12		49.2	9.73	2.08
TAPC	FMG	17	25.2	1.6	4.7	4.0	0.4		5.8	1.5	32.4	11.2	78.4	79	18.2	84	5.6		2.62	0.00	1.28	442	23.7	47.6	5.07	17.5	3.11	0.44	3.02		2.68		1.70		1.77	0.30	2.55		37.4	9.70	2.75
TAPC	FMG	19	21.1	0.5	7.5	2.2	0.3		3.3	0.6	25.7	9.6	145.2	65	20.6	100	4.2		1.30	0.01	1.79	864	29.6	56.3	6.27	22.6	4.05	0.65	3.69		3.78		2.67		2.88	0.48	3.12		33.6	8.35	1.68
TAPC	FMG	20	17.8	0.8	3.5	1.8	0.5		4.3	0.3	21.9	9.5	137.2	87	12.1	85	4.6		1.41	0.02	3.99	1199	28.8	51.4	5.49	19.6	3.32	0.64	2.71		2.16		1.52		2.00	0.33	2.72		40.8	8.37	2.39
TAPC	FMG	22	15.9	1.8	4.4	27.2	0.5		0.8	1.4	36.2	11.3	53.8	79	17.5	72	3.9		2.32	0.01	1.39	380	41.6	39.7	8.26	28.5	4.69	0.62	4.21		3.09		1.96		2.75	0.49	2.49		23.3	8.69	0.94
TAPC	FMG	23	30.1	1.7	6.8	10.0	0.6		1.2	1.9	22.8	12.2	87.0	110	10.2	92	3.7		1.22	0.02	2.74	453	19.4	45.6	3.94	14.2	2.61	0.42	2.13	0.31	1.94	0.40	1.33	0.25	2.00	0.36	2.90		15.4	7.62	1.15
TAPC	FMG	25	9.5	0.9	10.3	9.9	0.2		1.4	3.2	11.2	11.3	19.9	145	10.1	119	4.0		1.18	0.01	0.75	196	6.2	11.6	1.17	4.7	0.83	0.47	0.86		1.38		1.40		1.79	0.28	3.02		7.7	2.92	1.66
TAPC	FMG	26	45.0	1.9	8.2	12.8	0.9		2.5	0.4	21.0	12.1	85.6	149	20.4	88	4.3		1.13	0.01	2.09	529	32.8	66.7	6.76	24.8	4.63	0.79	4.61		4.11		2.05		1.73	0.28	3.23		21.0	8.56	1.32
TAPC	FMG	29	20.8	1.9	4.0	5.9	0.2		0.5	1.4	21.2	11.0	51.2	114	12.0	131	2.4		1.31	0.01	0.60	340	7.3	11.6	1.43	5.4	0.99	0.40	0.90		1.45		1.93		3.03	0.50	3.97		25.3	7.65	0.83
TAPC	FMG	33	29.3	2.2	6.7	7.3	0.2		2.9	1.2	20.5	13.6	59.2	90	7.3	106	5.1		1.93	0.04	3.45	100	5.3	9.4	1.12	4.1	0.85	0.44	0.91		1.13		0.85		0.99	0.17	4.53		19.8	1.34	1.84
TAPC	FMG	34	29.6	2.2	5.4	10.4	0.2		1.4	0.7	20.5	12.5	52.6	87	4.4	111	4.9		1.87	0.04	3.56	88	5.8	6.0	0.70	2.5	0.54	0.40	0.61		0.88		0.70		0.85	0.15	4.31		19.5	0.83	1.60
TAPC	FMG	36	19.3	1.9	12.7	22.2	0.4		2.3	1.0	18.9	13.2	36.4	115	29.9	77	3.6		1.62	0.01	2.85	178	19.6	38.1	4.41	17.8	3.87	0.71	4.51		6.08		4.55		5.25	0.82	3.96		15.3	6.32	3.59
TAPC	FMG	37	22.6	2.7	5.9	0.4	0.2		2.4	4.3	51.8	12.4	103.2	60	20.5	83	7.7		2.11	0.01	1.39	625	17.6	25.5	3.87	14.6	3.01	0.37	2.81		2.88		2.22		2.61	0.42	2.80		22.0	10.02	2.45
TAPC	FMG	38	27.7	3.5	6.7	27.9	0.7		4.3	0.5	41.7	13.2	99.7	105	11.2	70	4.4		1.76	0.01	2.80	289	20.2	42.1	3.27	11.0	2.02	0.39	2.02		1.78		1.20		1.45	0.25	2.18		21.5	10.26	2.07
TAPC	FMG	41	19.4	2.1	7.0	2.6	0.2		2.9	3.2	55.1	12.2	73.3	44	31.9	78	5.6		2.07	0.01	1.13	355	24.2	48.7	6.06	23.3	4.72	0.44	4.73		4.75		3.09		3.65	0.57	2.91		16.8	7.08	2.38
TAPC	FMG	42	12.6	1.6	5.9	1.5	0.1		0.5	0.2	23.1	12.0	85.0	47	32.7	91	4.3		0.87	0.00	0.65	494	14.2	32.4	3.19	11.7	2.69	0.53	3.48		6.59		5.52		6.50	1.05	4.22		18.1	9.44	3.66
TAPC	FMG	48	68.1	1.0	25.7	169.0	19.3		9.7	1.1	80.8	15.9	101.3	163	24.3	100	6.1		2.22	0.07	12.56	653	30.7	56.1	6.54	24.5	4.46	0.82	4.22		3.92		2.41		2.36	0.38	3.38		15.3	9.52	2.18

TABLE A3-2
(continued)

Body[1]	Rock[2]	Sample	Trace elements, ppm																																			
			Li	Be	Sc	V	Cr	Co	Ni	Cu	Zn	Ga	Rb	Sr	Y	Zr	Nb	Mo	Sn	Sb	Cs	Ba	La	Ce	Pr	Nd	Sm	Eu	Gd	Tb	Dy	Ho	Er	Tm	Yb	Lu	Hf	Ta	Pb	Th	U
TAPC	FMG	50	44.8	0.9	10.5	56.6	9.6		4.6	2.9	35.1	12.5	116.0	127	16.8	124	6.9		0.99	0.07	3.22	896	24.5	49.9	4.92	17.6	3.23	0.53	2.95	0.43	2.68	0.58	1.74	0.27	1.93	0.33	4.04		15.4	14.96	3.62
TAPC	FMG	51	35.4	1.0	14.5	92.6	12.7		6.2	9.9	36.7	14.3	114.0	206	17.2	104	5.7		1.65	0.13	5.11	848	22.1	42.2	4.63	17.0	3.31	0.72	2.95	0.45	2.76	0.59	1.71	0.27	1.91	0.31	3.10		10.8	12.58	3.82
TAPC	FMG	52	31.8	1.1	13.5	86.6	11.3		5.8	12.2	33.9	14.5	125.2	243	17.8	106	5.9		1.64	0.13	4.84	963	28.1	51.9	5.67	19.7	3.52	0.72	3.02	0.45	2.82	0.61	1.77	0.29	2.02	0.33	3.36		28.2	14.28	4.35
TAPC	FMG	53	44.8	1.2	20.2	82.5	8.9		3.7	4.1	64.2	16.8	87.7	192	31.5	143	7.6		1.28	0.01	4.74	660	24.9	57.0	6.10	24.1	5.24	1.04	5.06	0.83	5.20	1.13	3.17	0.48	3.12	0.49	4.24		12.9	8.39	6.31
TAPC	FMG	54	53.5	1.2	17.8	83.2	5.0		3.8	5.5	62.0	15.9	90.6	178	28.3	134	7.3		1.77	0.01	9.78	682	21.8	47.4	5.37	20.9	4.48	0.86	4.26	0.69	4.48	0.99	2.96	0.47	3.20	0.52	4.39		11.9	9.30	2.19
TAPC	FMG	55	39.4	1.6	17.4	83.5	5.9		8.8	1.7	89.0	16.3	121.4	143	32.4	144	7.8		2.03	0.05	10.98	922	29.5	58.9	7.04	27.3	5.80	1.01	5.37	0.85	5.36	1.16	3.30	0.51	3.38	0.54	4.75		23.2	9.58	2.49
TAPC	FMG	57	21.6	1.7	44.3	263.8	78.1		35.4	2.6	68.9	18.2	7.3	217	15.2	31	3.8		2.49	0.08	0.41	23	4.3	7.7	1.10	5.8	1.77	0.68	2.14		2.67		1.65		1.55	0.23	0.99		17.6	0.78	0.85
TAPC	FMG	58	16.5	0.9	56.4	396.6	1.2		12.7	35.0	82.8	17.5	3.6	317	25.7	64	4.0		1.61	0.14	0.14	59	11.1	26.1	3.79	16.8	3.82	0.89	4.20		4.70		2.89		2.87	0.46	2.17		11.5	2.44	0.74
TAPC	FMG	61	17.3	0.5	41.4	296.1	10.4		12.5	25.3	76.3	15.9	7.3	145	17.9	32	1.2		1.05	0.03	0.33	85	2.2	5.3	0.89	4.8	1.75	0.64	2.32		3.10		2.05		2.03	0.34	1.16		3.7	1.06	0.39
TAPC	FMG	62	53.2	1.1	51.0	239.6	130.6		46.8	44.1	75.9	14.8	14.2	165	12.3	23	1.0		2.83	0.06	1.10	60	4.5	9.6	1.17	5.5	1.58	0.55	1.75		2.13		1.34		1.37	0.21	0.78		4.9	1.79	0.50
TAPC	FMG	JB-06	27.7	0.3	52.0	404.9	79.9		20.8	16.5	80.8	15.1	11.3	120	10.5	11	0.7		0.20	0.03	0.21	50	3.3	5.4	0.81	3.6	1.02	0.35	1.35	0.23	1.58	0.36	1.01	0.16	1.04	0.18	0.41		6.8	0.55	0.50
TAPC	FMG	JB-13	21.1	1.7	3.7	1.8	0.5		0.9	0.4	25.2	12.2	151.1	52	18.1	75	6.1		1.59	0.02	4.18	713	37.1	70.8	7.80	27.2	5.13	0.54	4.32	0.58	3.33	0.65	1.88	0.31	2.21	0.39	2.77		45.8	11.48	2.71
Erving[3]	Amph	2	11.1	0.4	43.3	256.5	354.7	46.4	82.6	2.5	75.6	14.1	2.4	154	27.0	69	0.8	0.23		0.06	0.22	18	2.1	7.1	1.38	7.9	2.90	1.19	3.97	0.72	4.71	1.03	2.87	0.42	2.63	0.41	2.07	0.06	2.7	0.10	0.03
Erving[3]	Amph	5	41.0	0.4	40.7	252.1	383.1	45.8	99.3	62.9	65.3	15.4	2.8	142	26.8	67	0.8	0.12		0.17	0.41	21	2.6	7.7	1.45	8.2	2.84	1.13	3.85	0.69	4.49	0.98	2.76	0.41	2.50	0.40	1.94	0.06	7.4	0.13	0.14
Erving[3]	Amph	7	82.0	0.7	47.3	298.9	261.9	43.6	64.8	12.5	82.6	16.3	4.6	364	28.5	76	0.9	0.10		0.11	0.35	88	2.3	7.5	1.47	8.2	2.99	1.12	4.22	0.77	5.04	1.09	3.08	0.46	2.84	0.44	2.22	0.07	9.8	0.09	0.06
Erving[3]	Amph	9	11.3	0.3	45.2	171.7	303.9	41.1	113.1	66.2	37.1	11.7	3.7	160	12.2	20	0.4	0.06		0.06	2.38	14	1.3	2.6	0.59	3.1	1.17	0.61	1.74	0.32	2.13	0.47	1.28	0.19	1.13	0.18	0.65	0.03	2.4	0.05	0.02
Erving	Amph	BN-48	64.0	1.6	45.2	398.9	219.5	52.4	65.6	56.0	114.4	18.8	9.6	124	50.2	152	2.8	0.37	1.57	0.09	1.13	27	5.4	16.0	2.79	15.3	5.17	1.75	7.07	1.25	8.27	1.77	5.01	0.76	4.93	0.79	4.11	0.33	2.5	0.20	0.29
Erving	Amph	BN-49	13.1	0.8	42.7	337.2	169.1	47.1	58.5	44.5	90.5	17.3	4.7	455	40.4	116	2.0	0.26	1.10	0.12	0.23	94	4.8	13.0	2.27	12.3	4.12	1.42	5.63	1.00	6.61	1.42	3.97	0.60	4.00	0.63	3.17	0.28	6.0	0.18	0.29
Erving	Amph	BN-50	125.0	0.8	42.2	559.2	8.1	47.1	15.4	10.7	142.9	22.6	12.8	122	68.4	227	4.1	0.57	1.74	0.17	0.54	25	7.6	23.9	4.02	22.3	7.27	2.40	9.74	1.72	11.22	2.44	6.78	1.03	6.73	1.07	5.96	0.54	3.3	0.25	0.11
Erving	Amph	BN-51	115.8	0.7	44.3	379.2	120.6	48.3	54.3	69.1	107.4	18.8	104.5	177	47.6	149	2.8	0.17	1.33	0.22	25.14	220	5.6	16.5	2.77	15.2	5.01	1.65	6.73	1.18	7.77	1.66	4.61	0.70	4.55	0.72	3.94	0.35	9.2	0.31	0.19
Erving	Amph	BN-52	28.6	1.2	38.9	254.8	340.8	48.1	73.7	72.8	71.3	15.9	6.1	200	26.8	72	1.0	0.14	0.72	0.16	0.58	31	2.2	7.3	1.28	7.6	2.62	1.02	3.66	0.66	4.36	0.95	2.63	0.39	2.55	0.41	1.97	0.19	7.7	0.10	0.07
Erving	Amph	BN-53	49.4	0.2	35.8	223.9	355.8	47.8	108.4	53.9	64.8	14.4	7.6	126	22.5	50	0.6	0.13	0.53	0.13	1.75	29	1.5	5.1	0.95	5.7	2.10	0.82	3.03	0.55	3.67	0.79	2.20	0.33	2.15	0.34	1.51	0.13	2.8	0.05	0.05
BC	QzMzd	A13-A	18.6	2.0	14.2	92.7	192.2	19.6	95.3	22.3	56.9	19.9	98.4	1759	17.7	84	7.1	0.33	1.12		2.62	3528	105.3	208.2	24.15	91.3	13.49	3.18	7.69	0.85	3.84	0.61	1.47	0.19	1.16	0.18	2.59	0.46	53.4	24.86	4.05
BC	QzMzd	A13-B	22.3	2.0	15.8	112.8	205.9	23.4	110.3	29.6	68.0	21.0	96.0	1781	19.2	206	9.5	0.38	1.38		2.97	2306	109.4	213.0	24.68	94.5	14.60	3.48	8.29	0.89	3.99	0.66	1.49	0.21	1.28	0.19	5.17	0.44	45.6	29.14	4.07
BC	QzMzd	A13-C	23.9	2.0	15.6	113.9	213.2	23.4	112.6	11.6	68.1	20.6	100.1	1777	19.0	225	9.4	1.01	1.39		3.34	2550	110.7	210.4	25.25	95.2	14.83	3.57	8.60	0.90	4.15	0.67	1.57	0.21	1.32	0.20	5.70	0.47	47.8	29.54	4.48
BC	QzMzd	A21-11	22.0	2.0	16.6	108.5	232.8	24.6	111.8	38.1	74.0	21.5	67.2	1800	22.2	204	6.4	0.39	1.43		1.75	2522	121.1	242.7	28.63	110.7	17.90	4.05	10.37	1.10	4.84	0.76	1.82	0.24	1.44	0.21	5.10	0.28	51.5	19.69	2.59
BC	QzMzd	A22-2Aa	20.9	2.1	18.1	125.9	255.3	26.3	121.1	1.8	81.4	21.6	75.1	1835	23.0	161	6.8	0.46	1.52		2.04	2626	124.7	246.6	29.94	115.7	18.73	4.38	10.64	1.14	5.09	0.81	1.88	0.24	1.48	0.22	4.11	0.29	47.0	18.02	2.55
BC	T	A22-2Ab	3.1	1.4	5.4	29.7	17.4	5.8	17.7	0.8	25.1	18.1	20.8	1401	10.1	110	4.2	0.46	1.11		0.49	795	21.2	44.1	5.19	20.5	4.00	1.24	3.16	0.41	2.05	0.36	0.89	0.12	0.74	0.11	2.79	0.29	30.4	5.39	1.14
HP	TG	Rt2H1	33.6	2.2	15.0	79.8	67.3	14.6	37.4	25.1	93.3	22.8	132.2	200	33.2	280	16.1	0.90	0.50		2.78	533	42.7	88.6	10.68	42.0	8.86	1.73	7.45	1.09	6.42	1.25	3.32	0.49	3.13	0.46	7.63	0.89	23.7	13.12	2.93
HP	T	Rt2H2	38.4	2.7	14.9	144.9	104.2	24.0	56.2	22.0	151.9	26.0	90.6	879	36.2	694	35.0	1.70	2.53		1.12	1452	101.0	220.6	26.86	104.8	17.44	3.87	11.76	1.48	7.50	1.31	3.12	0.42	2.58	0.35	16.27	1.63	33.4	17.42	2.47

[1]Body abbreviations: PP, Prescott Peninsula; TAPC, Taconian arc plutonic complex; Erving, Erving Formation amphibolites; BC, Belchertown Complex; HP, Hardwick Pluton.
[2]Rock abbreviations: PG, Packard Gabbro; CG, Cooleyville Gneiss; FMG, Fourmile Gneiss; Amph, amphibolite; QzMzd, quartz monzodiorite; TG, garnet-bearing tonalite; T, tonalite.
[3]Sulfur by ICP-MS, oxygen mass-shift mode.

REFERENCES CITED

Aleinikoff, J. N., and Moench, R. H., 1987, U–Pb geochronology and Pb isotopic systematics of plutonic rocks in northern New Hampshire: Ensimatic vs. ensialic sources: Geological Society of America, Abstracts with Programs, v. 19, n. 1 , p. 1.

——— 1992, U–Pb zircon ages of the Ordovician Ammonoosuc Volcanics and related plutons near Littleton and Milan, New Hampshire: Geological Society of America, Abstracts with Programs, v. 24, n. 3 , p. 2.

Aleinikoff, J. N., Rankin, D. W., Moench, R. H., and Walsh, G. J., 2015, New SHRIMP U–Pb zircon ages for felsic Ammonoosuc Volcanics, northern NH–VT: Geological Society of America Abstracts with Programs, v. 47, n. 3, p. 41.

Ashwal, L. D., Leo, G. W., Robinson, P., Zartman, R. E., and Hall, D. J., 1979, The Belchertown quartz monzodiorite pluton, west-central Massachusetts: A syntectonic Acadian intrusion: American Journal of Science, v. 279, n. 8, p. 936–969, https://doi.org/10.2475/ajs.279.8.936

Billings, M. P., and Wilson, J. R., 1964, Chemical analyses of rocks and rock-minerals from New Hampshire: Mineral Resources Survey, Part XIX, New Hampshire Division of Economic Development, 103 p.

Boucot, A. J., and Arndt, R., 1960, Fossils of the Littleton Formation (Lower Devonian) of New Hampshire: United States Geological Survey Professional Paper 334-B, p. 41–51, https://doi.org/10.3133/pp334B

Boucot, A. J., and Thompson Jr., J. B., 1958, Late Lower Silurian fossils from sillimanite zone near Claremont, New Hampshire: Science, v. 128, n. 3320, p. 362–363, https://doi.org/10.1126/science.128.3320.362

——— 1963, Metamorphosed Silurian brachiopods from New Hampshire: GSA Bulletin, v. 74, n. 11, p. 1313–1334, https://doi.org/10.1130/0016-7606(1963)74[1313:MSBFNH]2.0.CO;2

Boucot, A. J., MacDonald, G. J. F., Milton, C., and Thompson Jr., J. B., 1958, Metamorphosed middle Paleozoic fossils from central Massachusetts, eastern Vermont, and western New Hampshire: GSA Bulletin, v. 69, n. 7, p. 855–864, https://doi.org/10.1130/0016-7606(1958)69[855:MMPFFC]2.0.CO;2

Braathen, A., Nordgulen, Ø., Osmundsen, P. -T., Andersen, T. B., Solli, A., and Roberts, D., 2000, Devonian, orogen-parallel, opposed extension in the Central Norwegian Caledonides: Geology, v. 28, n. 7, p. 615–618, https://doi.org/10.1130/0091-7613(2000)028<0615:DOPOEI>2.3.CO;2

Brown, S. R., Andrews, G. D. M., and Gibson, H. D., 2016, Corrugated architecture of the Okanagan Valley shear zone and the Shuswap metamorphic complex, Canadian Cordillera: Lithosphere, v. 8, n. 4, p. 412–421, http://dx.doi.org/10.1130/L524.1

Castillo, P. R., 2006, An overview of adakite petrogenesis: Chinese Science Bulletin, v. 51, n. 3, p. 257–268, http://dx.doi.org/10.1007/s11434-006-0257-7

Chapman, A. D., Saleeby, J. B., Wood, D. J., Paisecki, A., Kidder, S., Ducea, M. N., and Farley, K. A., 2012, Late Cretaceous gravitational collapse of the southern Sierra Nevada batholith, California: Geosphere, v. 8, n. 2, p. 314–341, http://dx.doi.org/10.1130/GES00740.1

Clark Jr., R. G., and Lyons, J. B., 1986, Petrogenesis of the Kinsman intrusive suite: peraluminous granitoids of western New Hampshire: Journal of Petrology, v. 27, n. 6, p. 1365–1373, https://doi.org/10.1093/petrology/27.6.1365

Cohen, K. M., Finney, S. C., Gibbard, P. L., and Fan, J. -X., 2013 (updated 2018), The ICS International Chronostratigraphic Chart: Episodes, v. 36, n. 3, p. 199–204.

Defant, M. J., and Drummond, M. S., 1990, Derivation of some modern arc magmas by melting of young subducted lithosphere: Nature, v. 347, p. 662–665, https://doi.org/10.1038/347662a0

Despaigne-Díaz, A. I., García-Casco, A., Govea, D. C., Jourdan, F., Wilde, S. A., and Trujillo, G. M., 2016, Twenty-five million years of subduction–accretion–exhumation during the late Cretaceous–Tertiary in the northwestern Caribbean: The Trinidad Dome, Escambray Complex, central Cuba: American Journal of Science, v. 316, n. 3, p. 203–240, http://dx.doi.org/10.2475/03.2016.01

Dorais, M. J., 2003, The petrogenesis and emplacement of the New Hampshire plutonic suite: American Journal of Science, v. 303, n. 5, p. 447–487, http://dx.doi.org/10.2475/ajs.303.5.447

Elbert, D. C., Harris, A. G., and Denkler, K. E., 1988, Earliest Devonian conodonts from marbles of the Fitch Formation, Bernardston Nappe, north-central Massachusetts: American Journal of Science, v. 288, n. 7, p. 684–700, https://doi.org/10.2475/ajs.288.7.684

Eusden Jr.,, J. D., and Barreiro, B., 1988, The timing of peak high-grade metamorphism in central-eastern New England: Maritime Sediments and Atlantic Geology, v. 24, n. 3, p. 241–255, https://doi.org/10.4138/1654

Eusden Jr., J. D., Anderson, K., Beaudry, E., Dupee, M., Larkin, R., Minor, J., and Welling, D., 2006, Domes, volcanics, refolded folds and granites: A transect from the Bronson Hill arc into the Central Maine cover, Northern Presidential Range, New Hampshire, *in* Gibson, D., Daly, J., and Reusch, D., editors, Guidebook for Field Trips in Western Maine: New England Intercollegiate Geological Conference, 98th Annual Meeting, University of Maine Farmington, ME, p. 167–180.

Eusden, J. D., Baker, S., Cargill, J., Divan, E., Hillenbrand, I., O'Sullivan, P., and Wheatcroft, A., 2017, Transect From the Migmatized Central Maine Belt to the Bronson Hill Anticlinorium, *in* Johnson, B., and Eusden, J. D., editors, Guidebook for Field Trips in Western Maine and Northern New Hampshire: New England Intercollegiate Geological Conference, 109th Annual Meeting, Bates College, p. 287–304, http://dx.doi.org/10.26780/2017.001.0016

Ewart, A., 1982, The mineralogy and petrology of Tertiary–Recent orogenic volcanic rocks: with special reference to the andesitic–basaltic compositional range, *in* Thorp, R. S., editor, Andesites: Orogenic Andesites and Related Rocks: New York, John Wiley and Sons, p. 25–95.

Fitz, T. J., 2002, Magmatism in an extensional setting within the Bronson Hill belt: The Chickwolnepy intrusions of northern New Hampshire, *in* Mitchell, C. E., and Jacobi, R. D. editors, Taconic Convergence–Orogen, Foredeep, and Cratonic Interactions: Physics and Chemistry of the Earth, v. 27, n. 1–3, p. 97–108, https://doi.org/10.1016/S1474-7065(01)00004-3

Hall, R., 2018, The subduction initiation stage of the Wilson cycle, *in* Wilson, R. W., Houseman, G. A., McCaffrey, K. J. W., Doré, A. G., and Buiter, S. J. H., editors, Fifty Years of the Wilson Cycle Concept in Plate Tectonics: Geological Society, London, Special Publications, v. 470, 23 p., http://dx.doi.org/10.1144/SP470.3

Halpin, D. L., ms, 1965, The geometry of folds and style of deformation in the Quabbin Hill area, Massachusetts: Amherst, Massachusetts, Department of Geology and Geography, University of Massachusetts, Amherst, M.S. thesis, 93 p.

Harris, A. G., Hatch Jr., N. L., and Dutro Jr., J. T., 1983, Late Silurian conodonts update the metamorphosed Fitch Formation, Littleton area, New Hampshire: American Journal of Science, v. 283, n. 7, p. 722–738, https://doi.org/10.2475/ajs.283.7.722

Hibbard, J. P., van Staal, C. R., Rankin, D. W., and Williams, H., 2006, Lithotectonic map of the Appalachian Orogen, Canada–United States of America: Geological Survey of Canada, Map 2096A, scale 1:1,500,000, 2 sheets.

Hodgkins, C. E., ms, 1985, Geochemistry and petrology of the Dry Hill Gneiss and related gneisses, Pelham Dome, central Massachusetts: Amherst, Massachusetts, University of Massachusetts, Amherst, Department of Geology and Geography, M.S. thesis, Contribution n. 48, 137 p.

Hollocher, K., ms, 1985, Geochemistry of Metamorphosed volcanic rocks in the Middle Ordovician Partridge Formation, and amphibole dehydration reactions in the high-grade metamorphic zones of central Massachusetts: Amherst, Massachusetts, University of Massachusetts, Amherst, Department of Geology and Geography, Ph. D. thesis, Contribution n. 56, 275 p.

——— 1987, Systematic retrograde metamorphism of sillimanite–staurolite schists, New Salem area, Massachusetts: GSA Bulletin, v. 98, n. 6, p. 621–634, https://doi.org/10.1130/0016-7606(1987)98<621:SRMOSS>2.0.CO;2

——— 1993, Geochemistry and origin of volcanics in the Ordovician Partridge Formation, Bronson Hill Anticlinorium, west-central Massachusetts: American Journal of Science, v. 293, p. 671–721.

Hollocher, K., Bull, J., and Robinson, P., 2002, Geochemistry of the metamorphosed Ordovician Taconian magmatic arc, Bronson Hill Anticlinorium, western New England: Physics and Chemistry of the Earth, v. 27, p. 5–45, http://dx.doi.org/10.1016/S1474-7065(01)00002-X.

Hollocher, K., Robinson, P., Walsh, E., and Terry, M. P., 2007, The Neoproterozoic Ottfjället dike swarm of the Middle Allochthon, traced geochemically into the Scandian hinterland, Western Gneiss Region, Norway: American Journal of Science, v. 307, n. 6, p. 901–953, http://dx.doi.org/10.2475/06.2007.02

Hollocher, K., Robinson, P., Seaman, K., and Walsh, E. O., 2016, Ordovician–early Silurian intrusive rocks in the northwest part of the Upper Allochthon, mid-Norway: Plutons of an Iapetan volcanic arc complex: American Journal of Science, v. 316, n. 10, p. 925–980, http://dx.doi.org/10.2475/10.2016.01

Hueber, F. M., Bothner, W. A., Hatch Jr., N. L., Finney, S. C., and Aleinikoff, J. N., 1990, Devonian plants from southern Quebec and northern New Hampshire and the age of the Connecticut Valley Trough: American Journal of Science, v. 290, n. 4, p. 360–395, https://doi.org/10.2475/ajs.290.4.360

Huet, B., Le Pourhiet, L., Labrousse, L., Burov, E., and Jolivet, L., 2011, Post-orogenic extension and metamorphic core complexes in a heterogeneous crust: The role of crustal layering inherited from collision. Application to the Cyclades (Aegean domain): Geophysical Journal International, v. 184, n. 2, p. 611–625, http://dx.doi.org/10.1111/j.1365-246X.2010.04849.x

Karabinos, P., Samson, S. D., Hepburn, J. C., and Stoll, H. M., 1998, Taconian orogeny in the New England Appalachians: Collision between Laurentia and the Shelburne Falls arc: Geology, v. 26, n. 3, p. 215–218, https://doi.org/10.1130/0091-7613(1998)026<0215:TOITNE>2.3.CO;2

Karabinos, P., Macdonald, F. A., and Crowley, J. L., 2017, Bridging the gap between the foreland and hinterland I: Geochronology and plate tectonic geometry of Ordovician magmatism and terrane accretion on the Laurentian margin of New England: American Journal of Science, v. 317, n. 5, p. 515–554, http://dx.doi.org/10.2475/05.2017.01

Kay, A., Hepburn, J. C., Kuiper, Y. D., and Baxter, E. F., 2017, Geochemical evidence for a Ganderian arc/back-arc remnant in the Nashoba Terrane, SE New England, USA: American Journal of Science, v. 317, n. 4, p. 413–448, http://dx.doi.org/10.2475/04.2017.01

Kim, J., and Jacobi, R. D., 1996, Geochemistry and tectonic implications of Hawley Formation meta-igneous units: Northwestern Massachusetts: American Journal of Science, v. 296, n. 10, p. 1126–1174, https://doi.org/10.2475/ajs.296.10.1126

Kohn, M. J., and Spear, F., 1999, Probing the depths of Oliverian magmas: Implications for Paleozoic tectonics in the northeastern United States: Geology, v. 27, n. 9, p. 803–806, https://doi.org/10.1130/0091-7613(1999)027<0803:PTDOOM>2.3.CO;2

LeBas, M. J., LeMaitre, R. W., Streckeisen, A., Zanettin, B., and the IUGS Subcommission on the Systematics of Igneous Rocks, 1986, A chemical classification of volcanic rocks based on the total alkali–silica diagram: Journal of Petrology, v. 27, n. 3, p. 745–750, https://doi.org/10.1093/petrology/27.3.745

Leo, G. W., 1985, Trondhjemite and metamorphosed quartz keratophyre tuff of the Ammonoosuc Volcanics (Ordovician), western New Hampshire and adjacent Vermont and Massachusetts: GSA Bulletin, v. 96, n. 12, p. 1493–1507, https://doi.org/10.1130/0016-7606(1985)96<1493:TAMQKT>2.0.CO;2

——— 1991, Oliverian domes, related plutonic rocks, and mantling Ammonoosuc Volcanics of the Bronson Hill anticlinorium, New England Appalachians: United States Geological Survey Professional Paper 1516, 92 p., 1 plate, https://doi.org/10.3133/pp1516

Leo, G. W., Zartman, R. E., and Brookins, D. G., 1984, Glastonbury gneiss and mantling rocks (a modified Oliverian dome) in south-central Massachusetts and north-central Connecticut: Geochemistry, petrogenesis, and radiometric age: United States Geological Survey Professional Paper 1295, 45 p., https://doi.org/10.3133/pp1295

Lyons, J. B., and Livingston, D. E., 1977, Rb–Sr age of the New Hampshire plutonic series: Geological Society of America Bulletin, v. 88, n. 12, p. 1808–1812, https://doi.org/10.1130/0016-7606(1977)88<1808:RAOTNH>2.0.CO;2

Lyons, J. B., Aleinikoff, J. N., and Zartman, R. E., 1986, Uranium–thorium–lead ages of the Highlandcroft Plutonic Suite, northern New England: American Journal of Science, v. 286, n. 6, p. 489–509, https://doi.org/10.2475/ajs.286.6.489

Lyons, J. B., Bothner, W. A., Moench, R. H., and Thompson Jr., J. B., 1997, Bedrock geologic map of New Hampshire: United States Geological Survey, scale 1:250,000, 2 sheets.

Makower J., ms, 1964, Geology of the Prescott Intrusive Complex: Amherst, Massachussetts, Department of Geology and Geography, University of Massachusetts, Amherst, M.S. thesis, 106 p., 1 plate.

Massey, M. A., Moecher, D. P., Walker, T. B., O'Brian, T. M., and Rohrer, L. P., 2017, The role and extent of dextral transpression and lateral escape on the post-Acadian tectonic evolution of south-central New England: American Journal of Science, v. 317, n. 1, p. 34–94, http://dx.doi.org/10.2475/01.2017.02

McDonough, W. F., and Sun, S., 1995, The composition of the Earth: Chemical Geology, v. 120, n. 3–4, p. 223–253, https://doi.org/10.1016/0009-2541(94)00140-4

Michener, S. R., ms, 1983, Bedrock geology of the Pelham-Shutesbury Syncline, Pelham Dome, west-central Massachusetts: Amherst, Massachusetts, Geology Department, University of Massachusetts, Amherst, M.S. thesis, Contribution n. 43, 101 p, 5 plates.

Moench, R. G., and Aleinikoff, J. N., 2003, Stratigraphy, geochronology, and accretionary terrane settings of two Bronson Hill arc sequences, northern New England: Physics and Chemistry of the Earth, v. 28, n. 1–3, p. 113–160, https://doi.org/10.1016/S1474-7065(03)00012-3

Moench, R. H., Boone, G. M., Bothner, W. A., Baudette, E. L., Hatch Jr., N. L., Hussey II, A. M., and Marvinney, R. G., 1995, Geologic map of the Sherbrooke–Lewiston area, Maine, New Hampshire, and Vermont, United States, and Quebec, Canada: U. S. Geological Survey, Miscellaneous Investigation Series, Map I-1898-D, 2 sheets, with pamphlet.

Morton, P. S., ms, 1985, Tectonic breccia of metamorphosed intrusive igneous rocks in an Acadian shear zone, Brooks Village, north-central Massachusetts: Amherst, Massachusetts, Department of Geology and Geography, University of Massachusetts, Amherst, M.S. thesis, Contribution n. 54, 43 p., 1 plate.

Osberg, P. H., Tull, J. F., Robinson, P., Han, R., and Butler, J. R., 1989, The Acadian orogen, *in* Hatcher Jr., D., Thomas, W. A., and Viele, G. W., editors., The Appalachian–Ouachita Orogen in the United States: Geological Society of America, Boulder, Colorado, The Geology of North America, v. F-2, p. 179–232, https://doi.org/10.1130/DNAG-GNA-F2.179

Osmundsen, P. T., Eide, E. A., Haabesland, N. E., Roberts, D., Andersen, T. B., Kendrick, M., Bingen, B., Braathen, A., and Redfield, T. F., 2006, Kinematics of the Høybakken detachment zone and the Møre–Trøndelag Fault Complex, central Norway: Journal of the Geological Society, London, v. 163, n. 2, p. 303–318, http://dx.doi.org/10.1144/0016-764904-129

Pearce, J. A., and Parkinson, I. J., 1993, Trace element models for mantle melting: Application to volcanic arc petrogenesis, *in* Prichard, H. M., Alabaster, T., Harris, N. B. W., and Neary, C. R., editors, Magmatic Processes and Plate Tectonics: Geological Society of London, Special Publications, v. 76, p. 373–403, https://doi.org/10.1144/GSL.SP.1993.076.01.19

Pearce, J. A., and Stern, R. J., 2006, Origin of back-arc basin magmas: Trace element and isotope perspectives, *in* Christie, D. M., Fisher, C. R., Lee, S. -M., and Givens, S., editors, Back-Arc Spreading Systems–Geological, Biological, Chemical, and Physical Interactions: American Geophysical Union, Geophysical Monograph Series, v. 166, p. 63–86, https://doi.org/10.1029/166GM06

Peterson, V. L., ms, 1992, Structure, petrology, and tectonic implications of highly strained rocks along the west margin of the Acadian granulite-facies high, south-central Massachusetts: Amherst, Massachusetts, Geology Department, University of Massachusetts, Amherst, Ph. D. thesis, Contribution n. 69, 73 p., 2 plates.

Rankin, D. W., and Tucker, R. D., 2000, Monroe fault truncated by Mesozoic (?) Connecticut Valley rift system at Bradford, VT; Relationship to the Piermont Allochthon: Geological Society of America Abstracts with Programs, v. 32, n. 1, p. A–67.

Rankin, D. W., Coish, R. A., Tucker, R. D., Peng, Z. X., Wilson, S. A., and Rouff, A. A., 2007, Silurian extension in the upper Connecticut Valley, United States and the origin of Middle Paleozoic basins in the Quebec embayment: American Journal of Science, v. 307, n. 1, p. 216–264, https://doi.org/10.2475/01.2007.07

Rankin, D. W., Tucker, R. D., and Amelin, Y., 2013, Reevaluation of the Piermont–Frontenac allochthon in the Upper Connecticut Valley: Restoration of a coherent Boundary Mountains–Bronson Hill stratigraphic sequence: GSA Bulletin, v. 125, n. 5–6, p. 998–1024, http://dx.doi.org/10.1130/B30590.1

Reagan, M. K., Ishizuka, O., Stern, R. J., Kelley, K. A., Ohara, Y., Blichert-Toft, J., Bloomer, S. H., Cash, J., Fryer, P., Hanan, B. B., Hickey-Vargas, R., Ishii, T., Kimura, J. -I., Peate, D. W., Rowe, M. C., and Woods, M., 2010, Fore-arc basalts and subduction initiation in the Izu–Bonin–Mariana system: Geochemistry, Geophysics, Geosystems, v. 11, n. 3, p. 1–17, http://dx.doi.org/10.1029/2009GC002871

Rey, P. F., Teyssier, C., Kruckenberg, S. C., and Whitney, D. L., 2011, Viscous collision in channel explains double domes in metamorphic core complexes: Geology, v. 39, n. 4, p. 387–390, http://dx.doi.org/10.1130/G31587.1

Robinson, P., ms, 1963, Gneiss Domes of the Orange Area, Massachusetts and New Hampshire: Cambridge, Massachusetts, Harvard University, Ph. D. thesis, 253 p.

——— 1979, Bronson Hill Anticlinorium and Merrimack Synclinorium in central Massachusetts, *in* Skehan, J. W., and Osberg, P. H., editors, The Caledonides in the U. S. A., Geological Excursions in the Northeast Appalachians: Weston, Massachusetts, International Geological Correlation Program, Project 27–Caledonide Orogen, Weston Observatory, Department of Geology and Geophysics, Boston College, p. 126–150.

——— 2003, Tectonic–stratigraphic–metamorphic perspective of the New England Caledonides, west-central

Massachusetts, *in* Brady, J. B., and Cheney, J. T., editors, Guidebook for Field Trips in the Five College Region: Amherst and Northampton, Massachusetts, New England Intercollegiate Geological Conference, 95th Annual Meeting, p. A1–A54.

——— 2009, Bedrock geologic map of the Orange 7.5-minute quadrangle, Massachusetts, and adjacent parts of the Athol and Millers Falls Quadrangles (digital map): Geological Survey of Massachusetts, Amherst, scale 1:24,000, 5 sheets.

——— 2011, Bedrock geologic map of the Mount Grace 7.5-minute quadrangle and southeastern 2/3 of the Northfield 7.5-minute quadrangle (digital map): Geological Survey of Massachusetts, Amherst, scale 1:24,000, 6 sheets.

——— 2012, Bedrock Geology of the Mount Grace Quadrangle, Massachusetts and Adjacent New Hampshire, *in* Thompson, P. J., and Thompson, T., editors, Guidebook to Field Trips in Western New Hampshire and Adjacent Vermont and Massachusetts: Newburry, New Hampshire, New England Intercollegiate Geological Conference, 104th Annual Meeting, p. 253–306.

——— 2017, Bedrock Geology of the Winsor Dam 7.5-minute Quadrangle, Massachusetts: Geological Survey of Massachusetts, Amherst, scale 1:24,000, 4 sheets.

Robinson, P., and Mabee, S.B ., 2016, Massachusetts Geological Society Quabbin Reservoir Field Trip: A Review of the Geology in and Adjacent to the Quabbin Reservoir Area, May 14, 2016: Massachusetts Geological Survey, Open-File Report 16-01, 44 p.

Robinson, P., and Tucker, R. D., 1992, A traverse across the "wild unknowns" of north-central Massachusetts from the Bronson Hill Anticlinorium to the Fitchburg plutons, *in* Robinson, P., and Brady, J. B., editors, Guidebook for Field Trips in the Connecticut Valley Region of Massachusetts and Adjacent States: Amherst, Massachusetts, New England Intercollegiate Geological Conference, 84th Annual Meeting, v. 2, p. 424–445.

——— 1996, The Bronson Hill magmatic arc, New England: myth and reality: Geological Society of America Abstracts with Programs, v. 28, n. 3, p. 94.

Robinson, P., Field, M. T., and Tucker, R. D., 1982, Stratigraphy and structure of the Ware–Barre area, central Massachusetts, *in* Joesten, R., and Quarrier, S. S., editors, Guidebook for Fieldtrips in Connecticut and South-Central Massachusetts: Storrs, Connecticut, New England Intercollegiate Geological Conference, 74th Annual Meeting, p. 341–373.

Robinson, P., Hatch, N. L., and Stanley, R. S., 1988, The Whately thrust: A structural solution to the stratigraphic dilemma of the Erving Formation: United States Geological Survey Professional Paper 1366–8, p. B1–B34.

Robinson, P., Tracy, R. J., Hollocher, K., Berry IV, H. N., and Thompson, J. A., 1989, Basement and cover in the Acadian metamorphic high of central Massachusetts, *in* Chamberlain, C. P., and Robinson, P., editors, Styles of Metamorphism with Depth in the Central Acadian High, New England: Amherst, Massachusetts, Department of Geology and Geography, Contribution n. 63, University of Massachusetts, Amherst, p. 69–140.

Robinson, P., Tucker, R. D., Bradley, D., Berry IV, H. N., and Osberg, P. H., 1998, Paleozoic orogens in New England: GFF, Journal of the Geological Society of Sweden, v. 120, p. 119–148, https://doi.org/10.1080/11035899801202119n.2

Robinson, P., Hollocher, K., Lucas, B., Tucker, R. D., Schumacher, J. C., and McEnroe, S. A., 2017, A major earliest Silurian low-angle detachment in the Bronson Hill magmatic arc, Massachusetts and SW New Hampshire: Geological Society of America Abstracts with Programs, v. 49, n. 6, http://dx.doi.org/10.1130/abs/2017AM-305231

Rodgers, J., 1985, Bedrock Geological Map of Connecticut: Connecticut Geological and Natural History Survey, Connecticut Natural Resources Atlas Series, scale 1:250,000, 2 sheets.

Schumacher, J. C., 1988, Stratigraphy and geochemistry of the Ammonoosuc Volcanics, central Massachusetts and southwestern New Hampshire: American Journal of Science, v. 288, n. 6, p. 619–663, https://doi.org/10.2475/ajs.288.6.619

Sevigny, J. H., and Hanson, G. N., 1993, Orogenic evolution of the New England Appalachians of southwestern Connecticut: GSA Bulletin, v. 105, n. 12, p. 1591–1605, https://doi.org/10.1130/0016-7606(1993)105<1591:OEOTNE>2.3.CO;2

Shearer, C. K., ms, 1985, Petrography, mineral chemistry and geochemistry of the Hardwick tonalite and associated igneous rocks, central Massachusetts: Amherst, Massachusetts, Department of Geology and Geography, University of Massachusetts, Amherst, Ph. D. thesis, Contribution n. 51, 210 p.

Shearer, C. K., and Robinson, P., 1988, Petrogenesis of metaluminous and peraluminous tonalites within the Merrimack Synclinorium: Hardwick tonalite, central Massachusetts: American Journal of Science, v. 288-A, p. 148–195.

Sioui, K., ms, 1990, Sulfide-rich zone in the Monson Gneiss–quantitative petrologic study of a pre-metamorphic sulfide alteration zone along the western margin of the Monson Gneiss: Amherst, Massachusetts, Department of Geology and Geography, University of Massachusetts, Amherst, M.S. thesis.

Stanley, R. S., and Ratcliffe, N. M., 1985, Tectonic synthesis of the Taconian Orogeny in western New England: GSA Bulletin, v. 96, n. 10, p. 1227–1250, https://doi.org/10.1130/0016-7606(1985)96<1227:TSOTTO>2.0.CO;2

Sun, S., and McDonough, W. F., 1989, Chemical and isotopic systematics of oceanic basalts: Implications for mantle composition and processing, *in* Saunders, A. D., and Norry, M. J., editors, Magmatism in the ocean basins: Geological Society, London, Special Publications, v. 42, p. 313–345, http://dx.doi.org/10.1144/GSL.SP.1989.042.01.19

Taira, A., 2001, Tectonic evolution of the Japanese island arc system: Annual Review of Earth and Planetary Science, v. 29, p. 109–134, http://dx.doi.org/10.1146/annurev.earth.29.1.109

Tatsumi, Y., 2008, Making continental crust: The sanukitoid connection: Chinese Science Bulletin, v. 53, n. 11, p. 1620–1633, https://doi.org/10.1007/s11434-008-0185-9

Thompson, M. D., Barr, S. M., and Grunow, A. M., 2012, Avalonian perspectives on Neoproterozoic paleogeography: Evidence from Sm–Nd isotope geochemistry and detrital zircon geochronology in SE New England, USA: GSA Bulletin, v. 124, n. 3–4, p. 517–531, http://dx.doi.org/10.1130/B30529.1

Tracy, R. J., Robinson, P., and Wolff, R. A., 1984, Metamorphosed ultramafic rocks in the Bronson Hill anticlinorium, central Massachusetts: American Journal of Science, v. 284, n. 5, p. 530–558, https://doi.org/10.2475/ajs.284.4-5.530

Tremblay, A., and Pinet, N., 2005, Diachronous supracrustal extension in an intraplate setting and the origin of the Connecticut Valley–Gaspé and Merrimack troughs, northern Appalachians: Geological Magazine, v. 124, n. 1, p. 7–22, http://dx.doi.org/10.1017/S001675680400038X

Tucker, R. D., and Robinson, P., 1990, Age and setting of the Bronson Hill magmatic arc: A re-evaluation based on U–Pb zircon ages in southern New England: GSA Bulletin, v. 102, n. 10, p. 1404–1419, https://doi.org/10.1130/0016-7606(1990)102<1404:AASOTB>2.3.CO;2

——— 1991, Age of inherited components in composite, single zircons from the Dry Hill Gneiss, central Massachusetts: evidence concerning the "basement" of the Bronson Hill magmatic arc: Geological Society of America Abstracts with Programs, v. 23, n. 1, p. 141.

——— 1995, U–Pb age of the Hardwick Pluton and pre- "dome-stage" pegmatite, Quabbin Reservoir, and their bearing on the "Acadian" Orogeny in central Massachusetts and adjacent New Hampshire: Geological Society of America Abstracts with Programs, v. 27, n. 6, p. 223–224.

Tucker, R. D., Osberg, P. H., and Berry IV, H. N., 2001, The Geology of a part of Acadia and the nature of the Acadian Orogeny across central and eastern Maine: American Journal of Science, v. 301, n. 3, p. 205–260, http://dx.doi.org/10.2475/ajs.301.3.205

Valley, P. M., and Walsh, G., 2013, New U–Pb zircon ages from the Bronson Hill Anticlinorium, west-central New Hampshire: Geological Society of America, Northeastern Section Meeting, Abstract 51-11.

Valley, P. M., Walsh, G., and McAleer, R. J., 2015, New U–Pb zircon ages from the Bronson Hill arc, west-central New Hampshire: Geological Society of America Abstracts with Programs, v. 23, n. 1, p. 141.

van Staal, C. R., Whalen, J. B., Valverde-Vaquero, P., Zagorevski, A., and Rogers, N., 2009, Pre-Carboniferous, episodic accretion-related, orogenesis along the Laurentian margin of the northern Appalachians, *in* Murphy, J. B., Keppie, J. D., and Hynes, A. J., editors., Ancient Orogens and Modern Analogues: Geological Society, London, Special Publications, v. 327, p. 271–316, http://dx.doi.org/10.1144/SP327.13

Van Wagner, K. J., ms, 2017, Petrogenesis and concentric zonation of the Belchertown intrusive complex, west-central Massachusetts: Amherst, Massachusetts, Department of Geosciences, University of Massachusetts, Amherst, M.S. thesis, 90 p.

Vetti, V. V., and Fossen, H., 2012, Origin of contrasting Devonian supradetachment basin types in the Scandinavian Caledonides: Geology, v. 40, n. 6, p. 571–574, http://dx.doi.org/10.1130/G32512.1

Walsh, G. J., Valley, P. M., Merschat, A. J., McAleer, R. J., Ratcliffe, N. M., Thompson, P. J., Holm-Denoma, C. S., Roden-Tice, J. K., Regan, S. P., and Aleinikoff, J. N., 2017, Tectonic evolution of the Connecticut Valley region in south-central Vermont and west-central New Hampshire: Geological Society of America, Northeastern Section Meeting, Abstract 43-4, http://dx.doi.org/10.1130/abs/2017NE-290895

Watts, B. G., Dorais, M. J., and Wintsch, R. P., 2000, Geochemistry of Early Devonian calc-alkaline plutons in the Merrimack Belt: Implications for mid-Paleozoic terrane relationships in the New England Appalachians: Atlantic Geology, v. 36, n. 2–3, p. 79–102, https://doi.org/10.4138/2013

Whattam, S. A., and Stern, R. J., 2011, The "subduction initiation rule": A key for linking ophiolites, intra-oceanic forearcs, and subduction initiation: Contributions to Mineralogy and Petrology, v. 162, n. 5, p. 1031–1045, http://dx.doi.org/10.1007/s00410-011-0638-z

Wintsch, R. P., Kunk, M. J., Boyd, J. L., and Aleinikoff, J. N., 2003, P–T–t paths and differential Alleghenian loading and uplift of the Bronson Hill terrane, south-central New England: American Journal of Science, v. 303, n. 5, p. 410–446, http://dx.doi.org/10.2475/ajs.303.5.410

Yaliniz, M. K., 2008, A geochemical attempt to distinguish forearc and back arc ophiolites from the "supra-subduction" central Anatolian ophiolites (Turkey) by comparison with modern oceanic analogues: Ofioliti, v. 33, n. 2, p. 119–129, https://doi.org/10.4454/ofioliti.v33i2.363

Zartman, R. E., and Leo, G. W., 1985, New radiometric ages on gneisses of the Oliverian domes in New Hampshire and Massachusetts: American Journal of Science, v. 285, n. 3, p. 267–280, https://doi.org/10.2475/ajs.285.3.267

Zen, E-an, editor, 1983, Bedrock Geologic Map of Massachusetts: United States Geological Survey, scale 1:250,000, 3 sheets.

Zellmer, G. F., Lizuka, M., Miyoshi, M., Tamura, Y., and Tatsumi, Y., 2012, Lower crustal H_2O controls on the formation of adakitic melts: Geology, v. 40, n. 6, p. 487–490, http://dx.doi.org/10.1130/G32912.1